AD-A284 299

ARMY RESEARCH LABORATORY
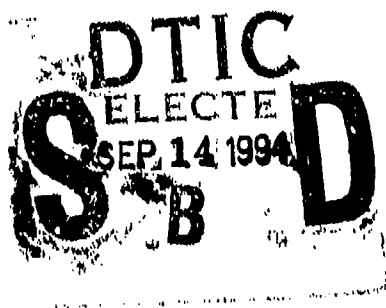
A Proposed Method for
Dynamic Analysis of Armored Structures:
Analytical Development and
Computer Simulation

Michael R. Sivack

ARL-TR-504   September 1994

DTIC
ELECTE
SEP 14 1994
S B D

94-29690

94 9 18 033

NOTICES

REPORT DOCUMENTATION PAGE

1. AGENCY USE ONLY (Leave blank)	2. REPORT DATE	3. REPORT TYPE AND DATES COVERED
	September 1994	Final, August 1991–December 1993

4. TITLE AND SUBTITLE

A Proposed Method for Dynamic Analysis of Armored Structures:
Analytical Development and Computer Simulation

5. FUNDING NUMBERS

4F592-462-63-V600

6. AUTHOR(S)

Michael R. Sivack

7. PERFORMING ORGANIZATION NAME(S) AND ADDRESS(ES)

U.S. Army Research Laboratory
ATTN: AMSRL-SL-BS
Aberdeen Proving Ground, MD 21005-5068

8. PERFORMING ORGANIZATION REPORT NUMBER

9. SPONSORING/MONITORING AGENCY NAME(S) AND ADDRESS(ES)

U.S. Army Research Laboratory
ATTN: AMSRL-OP-AP-L
Aberdeen Proving Ground, MD 21005-5066

10. SPONSORING/MONITORING AGENCY REPORT NUMBER

ARL-TR-504

11. SUPPLEMENTARY NOTES

12a. DISTRIBUTION/AVAILABILITY STATEMENT

Approved for public release; distribution is unlimited.

12b. DISTRIBUTION CODE

13. ABSTRACT (Maximum 200 words)

This report describes a simple proposed method for modeling and predicting ballistic shock effects with respect to biological damage and structural failure of an armored vehicle turret/hull interface. The research that forms the basis of this simplified approach is presented along with the limitations and advantages of this method. Assuming rigid body motion, an armored vehicle can be modeled as stacked blocks and equations of motion can be derived. The nonlinear, second order, differential equations are linearized then solved in general form and a mathematical analysis of the equations and their implications is presented.

DTIC QUALITY INSPECTED 3

14. SUBJECT TERMS

shock, nonlinear, dynamics, rigid body, transition blocks, moment of momentum

15. NUMBER OF PAGES

71

16. PRICE CODE

17. SECURITY CLASSIFICATION OF REPORT	18. SECURITY CLASSIFICATION OF THIS PAGE	19. SECURITY CLASSIFICATION OF ABSTRACT	20. LIMITATION OF ABSTRACT
UNCLASSIFIED	UNCLASSIFIED	UNCLASSIFIED	UL

INTENTIONALLY LEFT BLANK.

ACKNOWLEDGMENTS

iii

INTENTIONALLY LEFT BLANK.

TABLE OF CONTENTS

INTENTIONALLY LEFT BLANK.

LIST OF FIGURES

Intentionally left blank.

viii

LIST OF TABLES

INTENTIONALLY LEFT BLANK.

EXECUTIVE SUMMARY

Current vulnerability/lethality analysis methodology is concerned strictly with the local damage caused by penetration of KE penetrators or shaped charge jets. These damage mechanisms are of primary interest and have been extensively studied, both from a theoretical and a practical basis; however, another damage mechanism of considerable significance is ballistic shock. As tactical combat vehicles are becoming better protected against perforating impacts, the incidence of component and structure failure due to ballistic shock is becoming more significant in terms of the overall damage levels. Current methodology does not predict or account for these eff cts in a satisfactory and complete manner. This report will attempt to address one a ct of this complex problem as a genesis to the development of a suitable vulnerability/ lethality methodology that includes ballistic shock damage mechanisms.

Whereas the damage directly associated with the penetration event is considered local in nature, there can be global effects that degrade and incapacitate vehicle systems. These global effects arise from the forced vibratory loading due to the impact of the attacking munition. Such effects include far field structural failures, inoperable electro-optical devices and biological damage. As an initial assessment, this report will consider the gross motion of heavy structures subjected to nonperforating impacts (impulse loads) and what effect the structure interface has on the system dynamics. The structures are modeled as a single-degree-of-freedom (SDOF) system and a two-degree-of-freedom (2DOF) system to represent a turretless vehicle and a turreted vehicle, respectively. The turret and hull are idealized as rigid bodies connected together by a spring interface of variable stiffness. The dynamical equations of motion are derived under the condition of no slip and consist of two independent equations for each of the four main regimes of motion that the 2DOF system can occupy. The second order, ordinary differential equations are coupled and nonlinear. Analytic solutions are determined by linearizing and uncoupling the equations via modal analysis techniques. Due to physical discontinuities at the impact points, these analytical solutions are only valid in the continuous regimes of motion of the 2DOF system. Conservation of moment of momentum is used to derive transition equations that bridge these discontinuities by allowing the calculation of new initial conditions for the next regime of motion that the system enters. The local time histories of each regime of motion are then pieced together to yield the global dynamical response. By incorporating these analytical solutions within a FORTRAN computer simulation, the gross motion of the vehicles under varying impacts can be determined. A parametric study of the motion is performed by varying the stiffness of the turret interface and the physical properties of both the hull and turret. It is shown that system stability is a strong function of the mass and geometry and a weak function of the stiffness parameter. It is also shown that the mass of the turret has a strong damping effect on the motion of the hull due to the spring interface. This effect is more pronounced the stiffer the interface becomes. In general, it can be concluded that though the system stability is highly dependent on the mass and geometry of both the turret and hull, the effect of the stiffness associated with the turret interface can

stabilize the system under ceratin conditions and as the stiffness of the turret interface increases, the response of the 2DOF system becomes more like a rigid body, which is to be expected.

1. INTRODUCTION

With the advent of live-fire testing involving heavily armored structures, it has become apparent that damage mechanisms other than penetration and perforation have considerable significance in terms of munition lethality and target vulnerability. Specifically, ballistic shock effects have become more pronounced in terms of the overall damage levels sustained by armored targets during these tests, both for perforating and nonperforating impacts. Though the target damage assessment includes the effects associated with ballistic shock, current vulnerability and lethality analyses do not. In light of this situation, the U.S. Army has identified the need to better understand the ballistic shock phenomenon and to modify and upgrade current vunerability and lethality methodologies to satisfactorily address this issue.

An in-house research effort was initiated during the 1991 time frame by the U.S. Army Ballistic Research Laboratory (BRL), which was transitioned into the current U.S. Army Research Laboratory (ARL). The programmatic approach was to look at various ways to calculate and predict damage levels associated with ballistic shock and incorporate the most reasonable method within a current vulnerability methodology, with reasonable being defined as resource efficient, technically correct and answers that are simple and robust, so to speak. This report details the research efforts of one of the methods proposed to address certain areas within the overall ballistic shock program, the rigid body method (RBM). The author believes that this method has its greatest utility in addressing ballistic shock effects in terms of crew casualty predictions and assessments due to acceleration levels and structural failure of the turret-hull interface. Before discussing the research that forms the basis of the method in detail, it is appropriate to discuss shock in general and the applicability of this method.

Shock is generally defined as a relatively large force applied suddenly and quickly with a time period that is relatively short as compared to the natural period of the structure that is being subjected to this force. This transient force can produce damage local to the point of application of this force and also vibratory forces that affect the structure beyond the local point of application. These nonlocal effects are called the "global effects" and they are the focal point of this research effort.

The analytical technique termed "RBM" was investigated for a number of reasons. First and foremost, the assumptions associated with this method allow the use of some powerful mathematical techniques such as modal analysis, that, in conjunction with engineering dynamics, provide well-formulated equations of motion that are solvable either analytically or numerically. Secondly, this method should

1

provide the most conservative answer of the proposed methods in terms of structural survivability, thus setting an upper bound. Lastly, modeling of the physical system becomes relatively simple and unambiguous, requiring only computational algorithms and methods that are not time intensive. For these reasons, this method was investigated and the results generated using this method will be compared with empirical data generated from test programs when available.

A brief technical synopsis of this method and general vibration theory is presented here to facilitate a greater understanding and to present the advantages and limitations of this approach, as seen at this time. A structure, whether considered as a single component with isotropic material properties or as a conglomeration of components that may or may not share similar material properties, has associated with it a structural parameter called the natural frequency(s). The natural frequency, being a function of the material, geometry, and boundary conditions, is an inherent property of the structural system only, not any external conditions. Thus the natural frequency, or free vibration frequency, is the frequency or frequencies at which the structure oscillates after the external forcing function, i.e., the initiating impulse, is removed. This natural frequency (or frequencies) of a structure define the structure's response to external forces; i.e., when the structure is subjected to a broad-frequency acceleration environment such as an impact, the structure will absorb the energy more easily at certain frequencies, the natural frequencies of the system. So the acceleration response spectrum of the shock environment will have specific values at each natural frequency, the sum of which determines the total response of the structure. These acceleration values at each natural frequency specify the deformations and stresses induced in the structure with the lowest frequency referred to as the fundamental frequency. The greatest deformation, and therefore, the largest stresses and strains, occur at the fundamental frequency of the structure, in general. It is this fundamental frequency that we are interested in because it is associated with the largest peak acceleration values, and therefore, has the greatest potential for damage. If we can assume that the fundamental frequency of a real structure is close in magnitude to a similar structure modeled as a rigid-body, then this method should be useful.

This idealized assumption that the structure behaves as a rigid body requires that the structural stiffness or rigidity be high, or conversely, the structural damping approach zero since the damped frequency is defined as the natural frequency of a system with damping, or mathematically:

$$W_d = W_n \times \sqrt{1 - \zeta^2} \tag{1}$$

where
$\zeta = c / (2\, m\, W_n)$
W_d = damped frequency
W_n = natural frequency of system with no damping
m = mass
c = damping constant

2

Thus, when the damping constant c approaches zero, then the damped frequency approaches the natural frequency, as shown in equation 1. If we assume a structure composed of a very small number of components, we could determine the natural frequencies of each of these simple components, but we could not, in general, determine the natural frequencies of the structure from these individual frequencies. The structural frequencies are functions of the mass, stiffness, and damping of each component and the stiffness and damping asssociated with the interface between components. Thus to analyze anything but an extremely simple model requires a finite element analysis (FEA) program. So the following assumptions are necessary for rigid-body motion. The ratio of the stiffness of each individual component and their interfaces to the stiffness of an equivalent structure of homogeneous material should approach unity, where the stiffness is a function of material, material impedance at the interfaces, and structural rigidity. Thus the damping terms must approach zero or be very small compared to the total mass, as shown in equation 1. For an application of very heavy targets with rigidly welded plates, this assumption is considered reasonable at this time.

Assuming rigid-body motion, we can model an armored vehicle as a simple arrangement of two blocks connected by an equivalent spring constant representing the stiffness of the bolted turret/hull interface. This is a two-degree-of-freedom (2DOF) system requiring the solution of two simultaneous, second order, nonlinear, inertially and elastically coupled equations. This system can be solved two ways, either numerically or analytically. Analytic solutions for this problem were determined; though, in general there are very few known analytic solutions to nonlinear equations. In order to do this the nonlinear equations were linearized and then uncoupled using modal analysis techniques. This procedure allows for the relatively simple generation of analytic solutions for various forcing functions where the forcing function chosen is an analytic representation or model of the shock producing impact. The analytic representations under consideration for the forcing function are the Dirac delta function (actually a distribution) and a single pulse sine wave. Both of these functions were examined for derivation of the equations of motion but the system examined was the free vibration case since the purpose of this initial report is methodology development only. Development and validation of the specific forcing functions for ballistic shock modeling is currently being accomplished by the University of Dayton Research Institute (UDRI) as part of the overall shock program. Finally, one of the long term goals would be to solve the system of nonlinear equations numerically for comparison to the linear solutions.

The majority of research efforts dealing with rigid body motion lies in the field of civil/mechanical engineering, specifically, structural dynamics. A literature search was conducted and, though the relevant papers had strong civil orientations, the underlying physical and mathematical principles apply to this particularly military application.

The prevailing trend in structural dynamics is to assume that structures subjected to dynamic loads or excitations behave as a deformable continuum. There are

3

numerous examples of physical phenomena that, under certain conditions, contradict this assumption and, in fact, show that rigid body motion is a significant response mechanism. The collapse of the Cypress Street Viaduct (1880) during the 1989 Loma Prieta earthquake was kinematic in nature [1] and the Transamerica building exhibited a significant amount of rotation or rocking about its base [2] during the same event. Other examples of this rigid body behavior include the cyclic rocking, with the corresponding stretching of the base anchor bolts, of the relatively tall and slender petroleum cracking towers during the Arvin-Tehachapi earthquake, California, 21 July 1952 [3]. The primary reason for loss of structural integrity in these events was the rocking, and in some cases, subsequent toppling of these structures, and not due explicitly to some material failure mechanism. These events highlight the need for a better understanding of how structures undergoing rigid body motion respond to external stimuli.

The simplest way to model this behavior is by analyzing the rocking motion of a single rigid block on a rigid foundation. This has been done extensively in the literature, in recent times by Housner [3] and then expanded upon with variations to include flexible foundations of the two spring type [4] and the Winkler type [4,5,6], and both harmonic and random base excitations [7,8,9,10]. A comprehensive review of the research up to 1980 was compiled by Ishiyama [11] and is a good introduction to this field. A more recent paper by Lipscombe and Pellegrino [12] compares experimental data from single rocking blocks to predicted data from the theoretical models of such systems with some interesting insights and conclusions.

This characterization of a structure as a single rigid body, though desirable in terms of its simplicity, does not adequately address the complexities inherent in most typical man-made structures of interest. Thus a few researchers have extended the research from single-degree-of-freedom (SDOF) systems such as the single rocking block to multi-degree-of-freedom (MDOF) mechanisms, some as simple as two stacked blocks [13] and others as complex as multiple story structures composed of individual rigid bodies [14,15,16,17]. These researchers have considered systems of interest comprised of rigid bodies stacked upon each other with no provision for any type of fastening arrangement. These rigid body assemblies represent precast concrete building systems without considering any physical connection between the individual rigid bodies. This report will attempt to extend the understanding of the behavior of such structures by addressing the dynamics of a rigid body system whereby the rigid bodies are interconnected or fastened together with springs of variable resistance to model physical connectors such as reinforcing bars, bolted connections, or a turret/ hull interface. This report begins to address what effect the fasteners, geometry variations, and mass considerations have on the system dynamics.

One idealization of such a MDOF system can be made by considering two symmetrically stacked blocks interconnected by two springs where the top block can represent the turret of an armored vehicle with the bottom block representing the hull. The blocks are allowed to rotate about their edges and the coefficient of friction is

4

considered large enough to preclude any slip; thus, the poles of rotation can be thought of, in a kinematic sense, as a pin constraint. A mathematical model is developed for such a system and the resulting equations of motion are solved analytically. The solutions are encoded within a computer program and the time histories of the two blocks are examined with respect to parameter variations of the masses and spring constants.

Since the time histories are determined as functions of the absolute rotation angles of each block, and kinematic expressions can be derived for velocities and accelerations at any point of the rigid bodies as a function of these absolute coordinates, then the g-levels at any point can be determined to assess crew incapacitation values. Also, failure of the bolted interface between the hull and turret can be calculated for known material and geometry specifications. The modeling and derivations are presented next.

5

2. MATHEMATICAL MODELING

The first system to consider for simplicity and possible insights into more complex systems, is a single rigid block rocking on a horizontal surface with attached springs. The assumptions with this model are that the springs operate only in the linear elastic range and are massless. See Figure 1 below.

$2 a_1$ --> Height of Block B_1

$2 b_1$ --> Width of Block B_1

C_1 ----> Center of Mass

l_1, l_2 --> Distance from Block Center to Springs R_1 and R_2 respectively

H ----> Free Length of Springs R_1, R_2

h_1 ----> Height of Center of Mass

n_1 ----> Distance from Edge to Center of Mass

FIGURE 1 - Single Block with Springs R_1 and R_2

Now consider block B_1 with some initial angular displacement, as shown in Figure 2. Note that the block rocks about its corners P_1 and P_2, and, for the shown configuration, spring R_1 remains at a constant length while spring R_2 is in tension. The block will eventually rotate clockwise and impact the horizontal surface

6
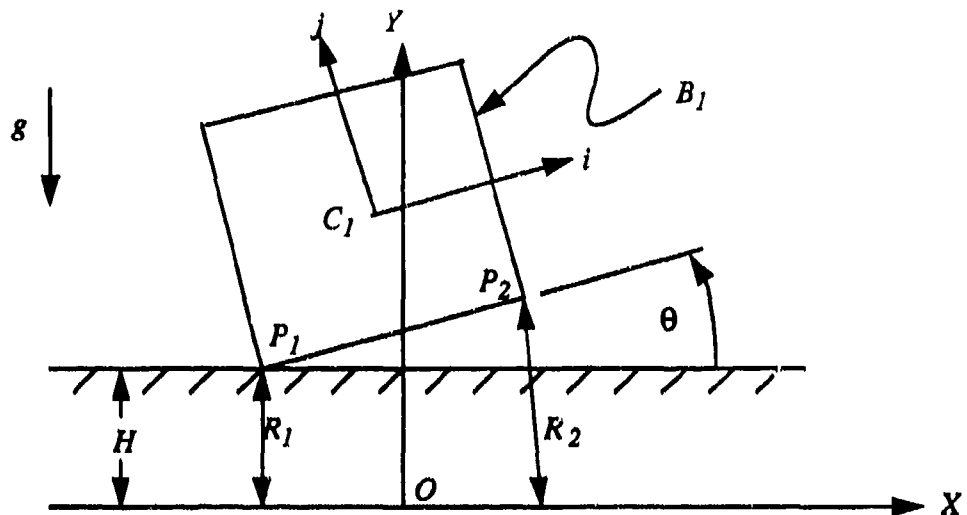
C_1 ----> Center of Mass
H ---- > Free Length of Springs R_1, R_2
K_1, K_2 ----> Spring Constants of Springs R_1 and R_2 respectively
L ----> Length of Springs R_1 and R_2, as an implicit function of θ

FIGURE 2 - Single Block with Displacement θ

and then begin to rotate about point P_2. It is this transition, from rocking about corner P_1 to rocking about corner P_2, that is one source of nonlinearity for this seemingly simple problem. Thus the equation of motion describing this rocking will be discontinuous at $\theta = 0$, which implies that the character of the equation will differ according to the sign of the angle of displacement, θ. Taking moments about points P_1 and P_2 gives the following equations of motion.

$$I_{P1}\,\ddot{\theta} + Mg\,(n_1 cos\theta - h_1 sin\theta) + K_2(1-H/L)(b_1+l_2)[Hcos\theta+(b_1+l_2)sin\theta]=0 \qquad (2a)$$

for $\theta > 0$ where $I_{P1} = I_{C1} + M(n_1^2 + h_1^2)$

$$I_{P2}\,\ddot{\theta} - Mg[(2\,b_1-n_1)cos\theta + h_1 sin\theta)] + K_1(1-H/L)(b_1+l_1)[Hcos\theta+(b_1+l_1)sin\theta]=0 \quad (2b)$$

for $\theta < 0$ where $I_{P2} = I_{C1} + M[(2\,b_1-n_1)^2 + h_1^2]$

These are the general forms of the equations of motion. If one assumes small displacements ($\theta < 20°$), a homogeneous distribution of mass, and that no gap exists between the ground and the reference frame ($H=0$), then the simplified equations are:

7

$$I_{P1}\ddot{\theta} + [K_2(b_1+l_2)^2 - Mga_1]\,\theta = -Mgb_1 \qquad \text{for } \theta > 0 \qquad (3a)$$

$$I_{P2}\ddot{\theta} + [K_1(b_1+l_1)^2 - Mga_1]\,\theta = Mgb_1 \qquad \text{for } \theta < 0 \qquad (3b)$$

An explanation concerning the validity of the previous assumptions is required at this time. One assumes small displacements in order to eliminate the nonlinearities associated with the trigonometric functions. Thus, the simplified equations are valid only as long as the rotation of the rocking block remains within the range of the small angular displacements. The second assumption concerning a homogeneous distribution of mass simply implies that the block's center of gravity coincides with the geometric center. This is a reasonable assumption for most man-made structures that would be considered as rigid body structures exhibiting the type of response this study addresses. The last assumption is more subtle than the other two and requires a more detailed explanation.

As stated earlier in this report, H represents the free length of the spring, but in actuality, it is only an artifact of how the system has been modeled. H could have been modeled as the distance from the horizontal base to the block, i.e., the increase in the length of the spring, with a spring free length of zero. This would effectively remove H from the equations since the spring force acting on the block is a function of θ only.

There are two important aspects or features that equations 3a and 3b bring to light for this relatively simple system which should hold true for more complex or MDOF systems also. The right-hand side (RHS) changes sign from equation 3a to equation 3b. This nonlinearity, mentioned previously, is due to the transition from rocking about one corner to the other corner. The second concerns the terms or coefficients associated with the displacement term, θ. The addition of the springs to the problem can change the character of the equations. If the spring constants K_1 and K_2 are set equal to zero, then the equations have negative stiffness. If the spring constants and certain physical parameters are great enough in magnitude, then it is possible for the equations to have positive stiffness. This is a significant feature which directly affects the form of the solution to these equations, as will be discussed next.

The solution set to equations 3a and 3b is presented below in equations 4a and 4b, respectively. Since the equations of motion are discontinuous at $\theta = 0$, a solution set is provided for both conditions, $\theta > 0$ and $\theta < 0$ by using the sgn function.

$$\theta(t) = D_1 \cos\sqrt{A}\,t + D_2 \sin\sqrt{A}\,t - (B/A)\,sgn\,\theta \qquad \text{for } A > 0 \qquad (4a)$$

$$\theta(t) = D_1 \cosh\sqrt{A}\,t + D_2 \sinh\sqrt{A}\,t + (B/A)\,sgn\,\theta \qquad \text{for } A < 0 \qquad (4b)$$

where $A = |A|$ since the sign of A is accounted for by the form of the solutions

and specifically: $A = [K_2(b_1+l_2)^2 - Mga_1] / I_{P1} = [K_1(b_1+l_1)^2 - Mga_1] / I_{P2}$

$$B = Mgb_1/I_{P1} = Mgb_1/I_{P2}$$

$$D_1 = \theta(0) + B/A \qquad D_2 = \dot{\theta}(0)/\sqrt{A} \qquad for \quad A > 0$$

$$D_1 = \theta(0) - B/A \qquad D_2 = \dot{\theta}(0)/\sqrt{A} \qquad for \quad A < 0$$

Thus it is evident that the sign of the displacement angle θ affects only the particular term of the total solution while the sign of the parameter A affects both the homogeneous part and the particular part of the total solution. The significance of this is that once the geometry of the block is defined then the sign of parameter A is determined by the value of the stiffness term K_i. The sign of A is determined by equation 5a and 5b presented below and as initially defined above.

$$A = [K_2(b_1+l_2)^2 - Mga_1] / I_{P1} \qquad for \quad \theta > 0 \qquad (5a)$$

$$A = [K_1(b_1+l_1)^2 - Mga_1] / I_{P2} \qquad for \quad \theta < 0 \qquad (5b)$$

By setting the parameter A to zero in equations 5a and 5b and solving for the K_i term, the threshold value for when the character of the solution changes from equation 4a to 4b or vice versa can be determined readily. These equations are presented next.

$$K_2 = Mga_1/(b_1+l_2)^2 \qquad for \quad \theta > 0 \qquad (6a)$$

$$K_1 = Mga_1/(b_1+l_1)^2 \qquad for \quad \theta < 0 \qquad (6b)$$

Thus, when the value of K_2 is greater than the value as determined in equation 6a then the solution is sinusoidal in nature, and, if less, the solution is hyperbolic in character. A similar statement can be made for the K_1 term. The practical significance of this phenomenon will be discussed in the results section of this report.

The nonlinearity due to transition of the block from the $\theta > 0$ case to the $\theta < 0$ case requires that the solution consist of two solutions, one from each of the linear regimes. Thus the total or global solution will consist of two local solutions which can be written in closed form due to the linear nature of the equations. This leads to an important consideration: how does the transition from rocking about one corner to rocking about the other corner affect the global solution? The two local solutions are

tied together by simply using the final conditions of the pre-impact or pre-transition regime as the initial conditions for the next regime. This implies that there is no energy loss during the transition and one would expect that the block would rock through an angle $\theta = -\theta_0$ where θ_0 is the initial displacement of the block (assuming no initial velocity). Therefore, the block would continue to rock forever for this conservative case of no energy dissipation. Practically, this case is not true, because during the transition, which is really an impact of the block with its supporting surface, there is an energy loss. In classical mechanics, this energy loss is accounted for by a proportionality constant (more formally known as a restitution coefficient, C,) that relates the pre-impact velocity to the post-impact velocity such as equation 7.

$$\dot{\theta}_f = C\,\dot{\theta}_i \qquad \text{where } 0 \le C \le 1 \qquad (7)$$

Equating the kinetic energy of the block immediately prior to impact and immediately after impact (since the potential energies are equivalent) with a proportionality factor, R, to account for the reduction in energy due to the impact gives equation 8.

$$\frac{1}{2}\,I_{P2}\,\dot{\theta}_f^2 = R\left(\frac{1}{2}\,I_{P1}\,\dot{\theta}_i^2\right) \qquad (8)$$

Realizing that $I_{P1} = I_{P2}$ for a homogeneous block, then the reduction in energy due to impact can be represented as R below.

$$R = \frac{\dot{\theta}_f^2}{\dot{\theta}_i^2} \qquad \text{i.e.,} \qquad R = C^2 \qquad (9)$$

Now, if the impact can be considered as perfectly plastic, i.e., the block does not bounce or slip, then the block's rotation is smooth and transits to the other pole of rotation in such a manner that conservation of angular momentum can be assumed. This assumption is pivotal in that it allows the derivation of an analytical expression relating the pre-impact and post-impact velocities to account for the discontinuity that occurs at $\theta = 0$. See the appendix for the derivation of the general equation for conservation of moment of momentum. Equating the moment of momentum about point P_1 immediately prior to impact and immediately after impact results in the following relationship.

$$I_{P1}\,\dot{\theta}_i - 2\,m\,b_1\,\dot{\theta}_i\,(b_1\cos\theta - a_1\sin\theta) = I_{P2}\dot{\theta}_f \quad \text{noting } I_{P1} = I_{P2} \qquad (10)$$

10

And since $\theta \approx 0$ during impact, equation 10 can be simplified with some rearranging.

$$C = \frac{\dot{\theta}_f}{\dot{\theta}_i} = 1 - \frac{3}{2}\left(\frac{b_1^2}{a_1^2 + b_1^2}\right) \quad (11)$$

What this equation implies is that even if one assumes the idealized conditions of a smooth transition from one pole of rotation to the other and rigid body conditions, there is going to be an energy loss during impact that is strictly a function of the geometry of the block! Thus, using equation 9, this energy loss can be represented as

$$\text{energy loss} = 1 - R \quad \text{or} \quad \text{energy loss} = 1 - C^2 \quad (12)$$

To minimize the energy loss during transition due to the block geometry, the last term of equation 11 must approach zero, which mathematically implies that $a_1 >> b_1$, i.e., tall, slender blocks. Conversely, short, wide blocks where $b_1 >> a_1$ corresponds to the maximum amount of energy loss. Recognizing that the theoretical lower limit of C is zero, it is a trivial exercise to show that this occurs when the ratio of b_1 to a_1 approaches the value 1.414 or $\sqrt{2}$. Also, it is interesting to note that if the ratio of b_1 to a_1 is less than 1.414, then C will be negative! Mathematically, this implies that the post-impact velocity is of opposite sign from the pre-impact velocity so there is a instantaneous change in the direction of rotation of the block. Physically, this means that the pole of rotation of the block does not change to the other corner, but that the block bounces back, maintaining the same pole of rotation. Practically, this does not occur and this condition implies that the block bounces, slips and leaves the surface of contact, thereby changing the scope of this problem and invalidating the assumption of conservation of moment of momentum. A recent paper by Lipscombe and Pellegrino [12] discusses this phenomenon in greater detail and concludes that the SDOF model with the assumption of conservation of moment of momentum is valid for slender blocks, but that this method is often inaccurate for short blocks where bouncing tends to be more pronounced. The paper also presents a comparison of experimental data for varying block geometries and three methods to model the phenomenon termed as "bouncing".

Although the condition represented by equation 6 with the theoretical limits of the proportionality factor C to model the impact or transition is necessary, it is not sufficient. By using the conservation of angular momentum principle, a more conservative estimate of the theoretical limits of C based on the geometry of the rigid body can be determined. This principle will also apply to more complex cases, as is discussed next.

The next step is to consider a more complex system or MDOF system (Figure 3), now that the relatively simpler system has provided some insights into the modeling
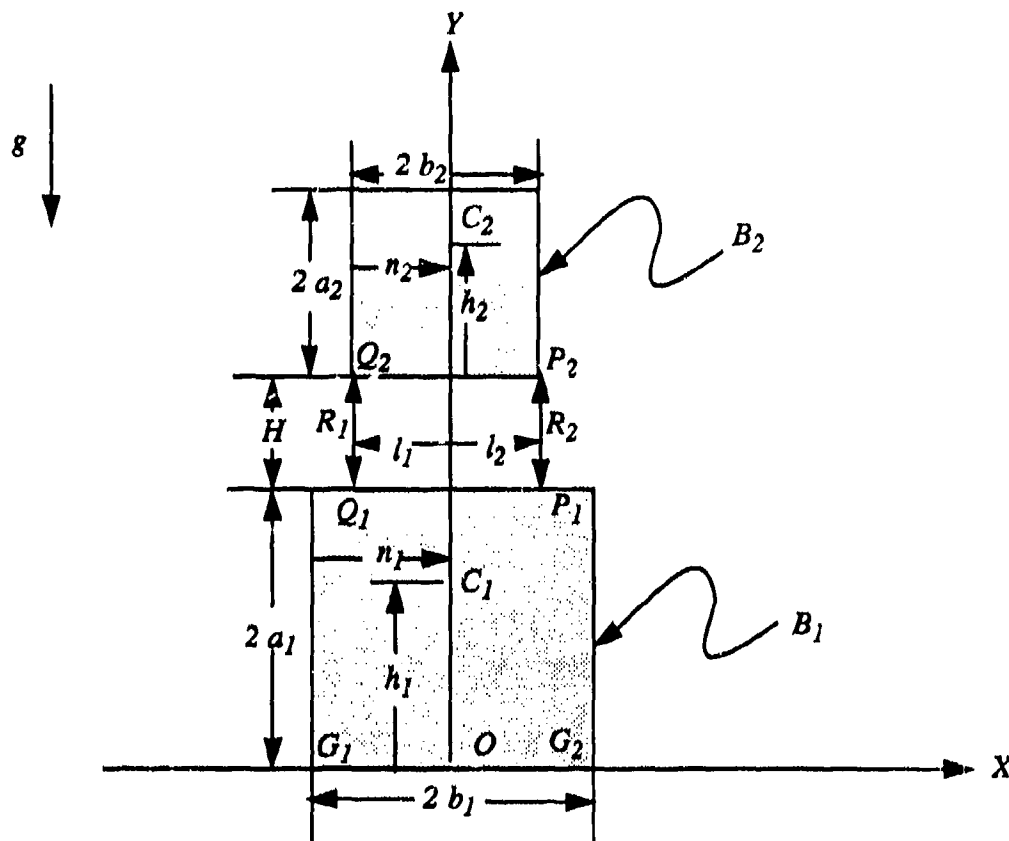
$2\,a_1$ --> Height of Block B_1 $\quad$ l_1, l_2 --> Distance from Block Center to Spring

$2\,b_1$ --> Width of Block B_1 $\quad$ h_1, h_2 -->Height of Center of Mass

$2\,a_2$ -->Height of Block B_2 $\quad$ n_1, n_2-->Distance from Edge to Center of Mass

$2\,b_2$ --> Width of Block B_2 $\quad$ R_1, R_2-->Springs R_1 and R_2

C_1-->Mass Center Block B_1 $\quad$ C_2-->Mass Center Block B_2

FIGURE 3 - Model of Two Stacked Blocks

and form of the equations of motion. This system consists of two blocks stacked together that are connected via springs and are placed on a rigid horizontal surface. All contact conditions are no-slip, the springs are massless and linear, and the system is subject to free vibration only, i.e., no external applied forces. The model of the system portrays the two blocks as separated by the length of the two springs but in actuality the system under consideration in this report has the blocks in direct contact. This was just done as a visualization aid during the modeling process. As with the single block model where this distance was represented by H, the same modeling artifice was used here and it is assumed that H is zero to get the correct equations for this particular model.

This system of two rocking blocks exhibits the same character as the single rocking block in the sense that the equations change when the displacement angles

12

change sign. This follows from the mathematical and physical discontinuity that occurs whenever either block transitions from rocking about one corner to rocking about the other corner. In addition, the point about which the top block rocks will not, in general, be stationary or fixed as it is for the bottom block; thus, there are Coriolis terms introduced into the final equations of motion. Furthermore, the motion of each block is highly dependent or coupled to the motion of the other block introducing further complexity into a seemingly simple problem. The aggregate effect of these system characteristics results in equations of motion that are highly nonlinear and atypical.

To make this problem more tractable, at least from a mathematical viewpoint, one must differentiate between the various regimes of motion that this system can possibly attain. Each regime of motion can be defined by the particular equation of motion that distinguishes one regime from another. It is somewhat obvious, especially considering the insights gained by the single rocking block problem, that this system can rock in at least four modes or phases, based on the geometry of the system and how the displacement angle sign changes occur. There are two other subphases that will be considered only as special cases of these four general phases. The four phases are presented in Figure 4.

The two special cases occur when both blocks rock in tandem (rigid body mode) and when only the top block rocks, which is simply the problem of the single rocking block discussed earlier. The only interest in the special case of both blocks rocking in concert, which once again can be considered as the single rocking block problem, is determining the conditions under which such a case can occur. That is not addressed in this report. The special case of the top block rocking only is essentially the problem of a single rocking block which has been studied extensively in the literature and will be considered only minimally in this report.

Cases 1 and 3 are similar except for the angular rotation direction and the same can be said for cases 2 and 4 in terms of their similarity. What this implies is that cases 1 and 3 will have the same form of the equations of motion except for a sign difference on the RHS of the equation, just like the single rocking block problem. Case 2 and 4 will exhibit the same characteristic, thus lending some efficiency to representing these equations in matrix form. Applying a Newtonian formulation to these models, the specific method used to derive the equations of motion is rather straightforward and is presented next.

To formulate two independent equations of motion for each of the four cases under consideration in this report the dynamic moments were equated to the sum of the moment of the forces. More specifically, it is possible to derive three equations of motion for this model, but only two equations are independent. There are also internal forces in this system due to the block-to-block contact and spring force that complicate the derivation. To simplify the derivation as much as possible, the first equation of motion was derived for the top block at its point of rocking with respect to the inertial

13
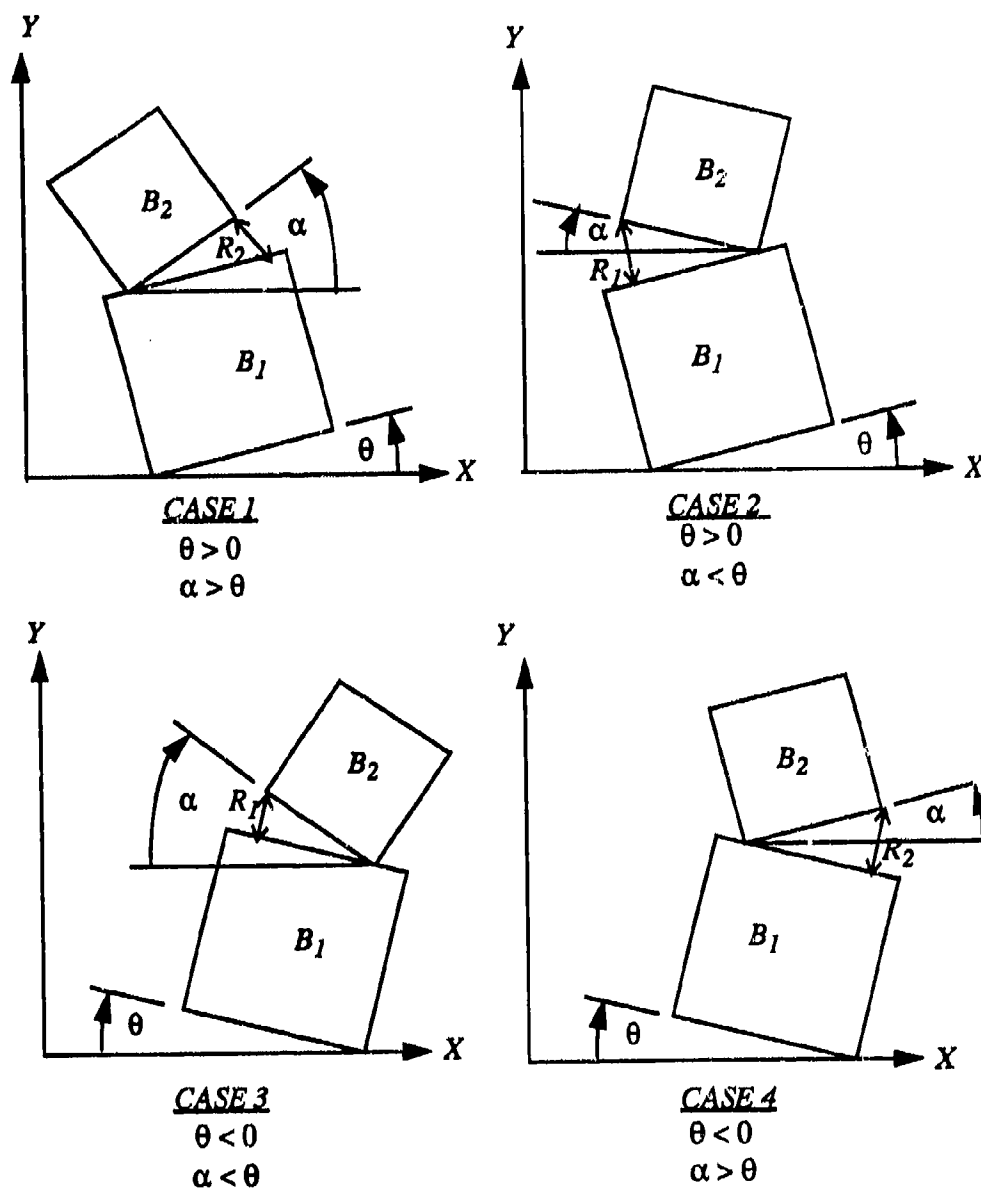
FIGURE 4 - Four Phases of Motion Under Consideration

reference frame ε. This alleviated the need to consider the block-to-block contact force since the moment of such a force about the point of application is always zero. However, since the point of block B_2 at which the moments are determined is not fixed with respect to the inertial reference frame, this must be accounted for when calculating the dynamic moment of this block and results in an expression that

includes some Coriolis terms. The second equation of motion was derived for block B_1 about the point of rocking for the system which, is coincident with the point of rocking for block B_1. This alleviated the need to consider the system contact force since the moment of such a force about the point of application is zero, as before. However, the spring force and the contact force due to the top block must be accounted for since, in general, the line of action of those forces will not pass through the point of application and, hence, their moments will not be zero. This results in one equation of motion per block for each of the four cases. Take case 1 for example (see Figure 4). Equation 12a is the result of taking the moment of the forces acting on block B_1 about point G_1 (see Figure 3), which is fixed in the inertial reference frame ε, and equating these forces to the dynamic moment of block B_1. The forces acting on block B_1 are: the weight of block B_1 in gravity field g, the spring force R_2 (always in tension), the contact force at point Q_1 due to block B_2, and the contact force of the system at point G_1. Since point Q_2 of block B_2 is coincident with point Q_1 of block B_1 there is no extension of spring R_1 so spring R_1 does not contribute to the dynamics of this particular case. Also, since the moments of the forces are being summed about point G_1 (which is fixed in the inertial reference frame ε for this specific case) the moment of the contact force at point G_1 is zero. Thus, the moments of the three remaining forces about point G_1 are equated to the dynamic moment of block B_1 about point G_1 to derive equation 12a. Since this is a 2DOF system, the second equation, equation 12b, is derived by evaluating the moments of the forces acting on block B_2 about its point of rocking, point Q_2, with respect to the inertial reference frame ε, and equating these moments with the dynamic moment of block B_2. The forces acting on block B_2 are: the weight of block B_2 in gravity field g, the spring force R_2, and the contact force at point Q_2 due to block B_1. Since point Q_2 of block B_2 is coincident with point Q_1 of block B_1, there is no extension of spring R_1, so spring R_1 does not contribute to the dynamics of this specific case. The moment of the contact force at point Q_2 is zero since it is being summed at the same point also. This same procedure is applied in the other three cases and the general equations are presented next.

CASE 1 --> $\theta > 0$, $\Gamma > \theta$

$$\{I_{B1C1} + m_1(n_1^2 + h_1^2) + m_2[(b_1 - l_1)^2 + (2a_1)^2]\}\ddot{\theta} \tag{13a}$$
$$-m_2\{[h_2(b_1-l_1)-2n_2a_1]\sin(\alpha-\theta) - [n_2(b_1-l_1)+2h_2a_1]\cos(\alpha-\theta)\}\ddot{\alpha}$$
$$-m_2\{[n_2(b_1-l_1)+2h_2a_1]\sin(\alpha-\theta) + [h_2(b_1-l_1)-2n_2a_1]\cos(\alpha-\theta)\}\dot{\alpha}^2$$
$$-[m_1h_1g+2m_2a_1g]\sin\theta - K_2(b_2+l_2)(l_1+l_2)\sin(\alpha-\theta) = -[m_1n_1g+m_2g(b_1-l_1)]\cos\theta$$

$$\{I_{B2C2} + m_2[n_2^2 + h_2^2]\}\ddot{\alpha} \tag{13b}$$
$$-m_2\{[h_2(b_1-l_1)-2n_2a_1]\sin(\alpha-\theta) - [n_2(b_1-l_1) + 2h_2a_1]\cos(\alpha-\theta)\}\ddot{\theta}$$
$$+m_2\{[n_2(b_1-l_1)+2h_2a_1]\sin(\alpha-\theta) + [h_2(b_1-l_1)-2n_2a_1]\cos(\alpha-\theta)\}\dot{\theta}^2$$
$$= -m_2g[n_2\cos\alpha - h_2\sin\alpha] - K_2(l_1+l_2)(b_2+l_2)\sin(\alpha-\theta)$$

15

$$\{I_{B1C1} + m_1(n_1^2+h_1^2) + m_2[(b_1+l_1)^2+(2a_1)^2]\}\ddot{\theta} \tag{14a}$$
$$-m_2\{[h_2(b_1+l_2)+2(2b_2-n_2)a_1]sin(\alpha-\theta)+[(2b_2-n_2)(b_1+l_2)-2h_2a_1]cos(\alpha-\theta)\}\ddot{\alpha}$$
$$+m_2\{[(2b_2-n_2)(b_1+l_2)-2h_2a_1]sin(\alpha-\theta)-[h_2(b_1+l_2)+2(2b_2-n_2)a_1]cos(\alpha-\theta)\}\dot{\alpha}^2$$
$$-K_1(b_2+l_1)(l_1+l_2)sin(\alpha-\theta)-(2m_2ga_1+m_1h_1g)sin\theta = -[m_1b_1g+m_2g(b_1+l_2)]cos\theta$$

$$\{I_{B2C2} + m_2[(2b_2-n_2)n_2 + h_2^2]\}\ddot{\alpha} \tag{14b}$$
$$-m_2\{[h_2(b_1+l_2)+2(2b_2-n_2)a_1]sin(\alpha-\theta)+[(2b_2-n_2)(b_1+l_2)-2h_2a_1]cos(\alpha-\theta)\}\ddot{\theta}$$
$$-m_2\{[2b_2-n_2)(b_1+l_2)-2h_2a_1]sin(\alpha-\theta)-[h_2(b_1+l_2)+2(2b_2-n_2)a_1]cos(\alpha-\theta)\}\dot{\theta}^2$$
$$= m_2g[b_2cos\alpha+h_2sin\alpha] - K_1(b_2+l_1)(l_1+l_2)sin(\alpha-\theta)$$

$$\{I_{B1C1}+m_1[(2b_1-n_1)^2+h_1^2]+m_2[(b_1-l_2)^2+(2a_1)^2]\}\ddot{\theta} \tag{15a}$$
$$+m_2\{[h_2(b_1-l_2)-2(2b_2-n_2)a_1]sin(\alpha-\theta)+[(2b_2-n_2)(b_1-l_2)+2h_2a_1]cos(\alpha-\theta)\}\ddot{\alpha}$$
$$-m_2\{[(2b_2-n_2)(b_1-l_2)+2h_2a_1]sin(\alpha-\theta)-[h_2(b_1-l_2)-2(2b_2-n_2)a_1]cos(\alpha-\theta)\}\dot{\alpha}^2$$
$$-K_1(b_2+l_1)(l_1+l_2)sin(\alpha-\theta)-[m_1h_1g+2m_2a_1g]sin\theta = [m_1g(2b_1-n_1)+m_2g(b_1-l_2)]cos\theta$$

$$\{I_{B2C2}+m_2[(2b_2-n_2)^2+h_2^2]\}\ddot{\alpha} \tag{15b}$$
$$+m_2\{[h_2(b_1-l_2)-2(2b_2-n_2)a_1]sin(\alpha-\theta)+[(2b_2-n_2)(b_1-l_2)+2h_2a_1]cos(\alpha-\theta)\}\ddot{\theta}$$
$$+m_2\{[(2b_2-n_2)(b_1-l_2)+2h_2a_1]sin(\alpha-\theta)-[h_2(b_1-l_2)-2(2b_2-n_2)a_1]cos(\alpha-\theta)\}\dot{\theta}^2$$
$$= m_2g[(2b_2-n_2)cos\alpha+h_2sin\alpha] - K_1(b_2+l_1)(l_1+l_2)sin(\alpha-\theta)$$

$$\{I_{B1C1}+m_1[(2b_1-n_1)^2+h_1^2]+m_2[(b_1+l_1)^2+(2a_1)^2]\}\ddot{\theta} \tag{16a}$$
$$+m_2\{[h_2(b_1+l_1)+2n_2a_1]sin(\alpha-\theta)-[n_2(b_1+l_1)-2h_2a_1]cos(\alpha-\theta)\}\ddot{\alpha}$$
$$+m_2\{[n_2(b_1+l_1)-2h_2a_1]sin(\alpha-\theta)+[h_2(b_1+l_1)+2n_2a_1]cos(\alpha-\theta)\}\dot{\alpha}^2$$
$$-K_2(b_2+l_2)(l_1+l_2)sin(\alpha-\theta)-[m_1h_1g+2m_2a_1g]sin\theta = [m_1b_1g+m_2g(b_1+l_1)]cos\theta$$

$$\{I_{B2C2}+m_2(n_2^2+h_2^2)\}\ddot{\alpha} \tag{16b}$$
$$+m_2\{[h_2(b_1+l_1)+2n_2a_1]sin(\alpha-\theta)-[n_2(b_1+l_1)-2h_2a_1]cos(\alpha-\theta)\}\ddot{\theta}$$
$$-m_2\{[n_2(b_1+l_1)-2h_2a_1]sin(\alpha-\theta)+[h_2(b_1+l_1)+2n_2a_1]cos(\alpha-\theta)\}\dot{\theta}^2$$
$$= m_2g[h_2sin\alpha-n_2cos\alpha]-K_2(b_2+l_2)(l_1+l_2)sin(\alpha-\theta)$$

where I_{B1C1} and I_{B2C2} are mass moments of inertia of each block about their respective centers of mass. Note that equation (a) refers to the equation of motion for block B_1 and equation (b) refers to the equation of motion for block B_2. Also note that a single equation of motion for the whole system can be derived and would just consist of the sum of equations (a) and (b), which is to be expected.

These are the general form of the equations of motion and they are extremely nonlinear so some simplifying assumptions are desired to make these equations more tractable. As before, assume a homogeneous distribution of mass, small angular displacements and that the connecting springs are located symmetrically about thevertical axis of each block. The equations are presented next.

CASE 1 --> $\theta > 0$, $\alpha > \theta$

$$\{I_{B1C1}+m_1[b_1^2+a_1^2]+m_2[(b_1-l_1)^2+(2a_1)^2]\}\ddot{\theta} + m_2[b_2(b_1-l_1)+2a_2a_1]\ddot{\alpha}$$
$$- K_2(b_2+l_2)(l_1+l_2)\alpha - [m_1a_1g+2m_2a_1g)-K_2(b_2+l_2)(l_1+l_2)]\theta$$
$$= -[m_1b_1g+m_2g(b_1-l_1)]$$
(17a)

$$m_2[b_2(b_1-l_1)+2a_2a_1]\ddot{\theta} + \{I_{B2C2}+m_2[b_2^2+a_2^2]\}\ddot{\alpha}$$
$$-[m_2a_2g-K_2(b_2+l_2)(l_1+l_2)]\alpha - K_2(b_2+l_2)(l_1+l_2)\theta = -m_2b_2g$$
(17b)

CASE 2 --> $\theta > 0$, $\alpha < \theta$

$$\{I_{B1C1}+m_1(b_1^2+a_1^2)+m_2[(b_1+l_1)^2+(2a_1)^2]\}\ddot{\theta}-m_2[b_2(b_1+l_2)-2a_2a_1]\ddot{\alpha}$$
$$-[m_1a_1g+2m_2a_1g-K_1(b_2+l_1)(l_1+l_2)]\theta-K_1(b_2+l_1)(l_1+l_2)\alpha=-[m_1b_1g+m_2(b_1+l_2)]$$
(18a)

$$-m_2[b_2(b_1+l_2)-2a_2a_1]\ddot{\theta} + \{I_{B2C2}+m_2(b_2^2+a_2^2)\}\ddot{\alpha} - K_1(b_2+l_1)(l_1+l_2)\theta$$
$$-[m_2a_2g-K_1(b_2+l_1)(l_1+l_2)]\alpha = m_2b_2g$$
(18b)

CASE 3 --> $\theta < 0$, $\alpha < \theta$

$$\{I_{B1C1}+m_1[b_1^2+a_1^2]+m_2[(b_1-l_1)^2+(2a_1)^2]\}\ddot{\theta}+ m_2\{b_2(b_1-l_2)+2a_2a_1\}\ddot{\alpha}$$
$$- [m_1a_1g+2m_2a_1g-K_1(b_2+l_1)(l_1+l_2)]\theta - K_1(b_2+l_1)(l_1+l_2)\alpha = m_1b_1g+m_2g(b_1-l_2)$$
(19a)

$$m_2[b_2(b_1-l_2)+2a_2a_1]\ddot{\theta} + \{I_{B2C2}+m_2[b_2^2+a_2^2]\}\ddot{\alpha} - K_1(b_2+l_1)(l_1+l_2)\theta$$
$$- [m_2a_2g-K_1(b_2+l_1)(l_1+l_2)]\alpha = m_2b_2g$$
(19b)

CASE 4 --> $\theta < 0$, $\alpha > \theta$

$$\{I_{B1C1}+m_1[b_1^2+a_1^2]+m_2[(b_1+l_1)^2+(2a_1)^2]\}\ddot{\theta} - m_2[b_2(b_1+l_1)-2a_2a_1]\ddot{\alpha}$$
$$- [m_1a_1g+2m_2a_1g-K_2(b_2+l_2)(l_1+l_2)]\theta- K_2(b_2+l_2)(l_1+l_2)\alpha =m_1b_1g+m_2g(b_1+l_1)$$
(20a)

$$- m_2[b_2(b_1+l_1)-2a_2a_1]\ddot{\theta} + [I_{B2C2}+m_2(b_2^2+a_2^2)]\ddot{\alpha} - K_2(b_2+l_2)(l_1+l_2)\theta$$
$$- [m_2a_2g-K_2(b_2+l_2)(l_1+l_2)]\alpha = -m_2b_2g$$
(20b)

To better visualize the similarities between the equations, they are presented next in matrix form, which lends a better understanding of their symmetry. First, some simple substitutions will be made for conciseness.

Let
$$I_G = I_{B1C1} + m_1[b_1^2 + a_1^2]$$
$$I_Q = I_{B2C2} + m_2[b_2^2 + a_2^2]$$
$$A = [b_2(b_1-l_1)+2a_2a_1] = [b_2(b_1-l_2)+2a_2a_1]$$
$$B = [b_2(b_1+l_2)-2a_2a_1] = \{b_2(b_1+l_1)-2a_2a_1]$$
since $l_1 = l_2$ because of symmetric spring placement.
$$K_{S1} = K_1(b_2+l_1)(l_1+l_2)$$
$$K_{S2} = K_2(b_2+l_2)(l_1+l_2)$$

The first matrix equation corresponds to cases 1 and 3 where the equations are the equations for each individual block, i.e., equations (a) and (b). As mentioned previously, the only difference between cases 1 and 3 is the sign change on the RHS. This is accounted for by using the sgn function, as shown below. The same nomenclature applies to the second matrix equation, which represents cases 2 and 4. The resulting equations are presented next.

CASE 1 --> $\theta > 0$, $\alpha > \theta$ and CASE 3 --> $\theta > 0$, $\alpha < \theta$

$$\begin{bmatrix} I_G + m_2[(b_1-l_1)^2+(2a_1)^2] & m_2A \\ m_2A & I_Q \end{bmatrix} \begin{bmatrix} \ddot{\theta} \\ \ddot{\alpha} \end{bmatrix} + \begin{bmatrix} K_{S2} - m_1a_1g - 2m_2a_1g & -K_{S2} \\ -K_{S2} & K_{S2} - m_2a_2g \end{bmatrix} \begin{bmatrix} \theta \\ \alpha \end{bmatrix}$$

$$= \begin{bmatrix} [m_1b_1g + m_2g(b_1-l_1)]sgn\,(\theta-\alpha) \\ [m_2b_2g]\,sgn\,(\theta-\alpha) \end{bmatrix}$$

CASE 2 --> $\theta < 0$, $\alpha < \theta$ and CASE 4 --> $\theta < 0$, $\alpha > \theta$

$$\begin{bmatrix} I_G + m_2[(b_1+l_2)^2+(2a_1)^2] & -m_2B \\ -m_2B & I_Q \end{bmatrix} \begin{bmatrix} \ddot{\theta} \\ \ddot{\alpha} \end{bmatrix} + \begin{bmatrix} K_{S1} - m_1a_1g - 2m_2a_1g & -K_{S1} \\ -K_{S1} & K_{S1} - m_2a_2g \end{bmatrix} \begin{bmatrix} \theta \\ \alpha \end{bmatrix}$$

$$= \begin{bmatrix} -[m_1b_1g + m_2g(b_1+l_2]\,sgn\,(\theta-\alpha) \\ [m_2b_2g]\,sgn\,(\theta-\alpha) \end{bmatrix}$$

In this form, the symmetry between the cases is readily apparent and facilitates the understanding, determination and encoding of a solution method. This system of local linearized equations is globally nonlinear due to the discontinuities at transition. However, valid and piecewise analytical solutions can be found in closed form between transitions. The method to do so and the solutions are presented in section 3.

18

3. ANALYTIC METHOD AND SOLUTIONS

As shown in the previous section, the nonlinear equations of motion (Eqs. 13 through 16) in their most general form, with the addition of an arbitrary forcing function $f(t)$, can be represented by

$$[I(\eta)]\{\ddot{\eta}\} + [J(\eta)]\{\dot{\eta}^2\} + [K]\{L(\eta)\} = [R]\{S(\eta)\}f(t) \qquad (21)$$

where the matrices $I, J, K,$ and R are coefficient matrices that are defined by the physical parameters of the system of interest and the vectors L and S are discontinuous functions of the original coordinates η_i, i.e., $\eta_1 = \theta$ and $\eta_2 = \alpha$. The forcing function, $f(t)$, is a general deterministic or probabilistic one and can include horizontal and vertical components of some ground excitation, or lateral excitation due to impact, wind, or other effects. As mentioned previously, these equations are nonlinear with specific nonlinear terms arising from Coriolis effects and geometrical constraints, that contribute trigonometric terms to the vectors L and S. The equations are nonautonomous under forced vibration. In addition, the matrices K and R undergo characteristic changes based on the sign of the original coordinates. As a result, there are N equations to describe N degrees of freedom with 2^N possible solution sets depending on the system parameters. Even after a linearization process by assuming small angles of rotation, atypical equations remain. Specifically, the resulting stiffness can be negative and, by virtue of the discontinuities, the systems of equations are only piecewise linear.

This equation, in its present form, does not have any known analytic solution but can be solved by a number of numerical techniques. Instead of solving the equations numerically, the equations will be linearized and piecewise analytic solutions will then be determined for the free vibration problem.

After linearization about $\theta = 0$ and $\alpha = 0$, and setting the forcing function $f(t)$ equal to zero, the system of equations become

$$[I]\{\ddot{\eta}\} + [K]\{\eta\} = \{Q\} \qquad \qquad (22)$$

where the vector Q, independent of time, represents a geometrical constraint due to the linearization process and not due to the general forcing function. Now, in general,

19

these equations are inertially and elastically coupled. Utilization of modal mathematical techniques will allow uncoupling the I and K matrices thereby allowing a solution set to be determined for this system.

Consider a linear transformation which maps the original coordinate system $\{\eta\}$ into a set of general coordinates $\{\theta\}$ as shown below. Using

$$\{\eta\} = [U]\{q\} \tag{23}$$

where matrix U is the transformation or modal matrix and the vector q represents the new or generalized coordinates allows the transformation of equation 22 to

$$[I][U]\{\ddot{q}\} + [K][U]\{q\} = \{Q\} \tag{24}$$

Now, pre-multiply through equation 24 by the transpose of matrix U which gives

$$[U]^T[I][U]\{\ddot{q}\} + [U]^T[K][U]\{q\} = [U]^T\{Q\} \tag{25}$$

Now allowing some straightforward substitutions for conciseness, equation 25 becomes

$$[m]\{\ddot{q}\} + [k]\{q\} = \{z\} \tag{26}$$

where
$$[m] = [U]^T[I][U]$$
$$[k] = [U]^T[K][U]$$
$$\{z\} = [U]^T\{Q\}$$

The object of these mathematical manipulations is to uncouple the original system of equations. This is accomplished by what is more commonly known as diagonalizing the original coefficient matrices I and K simultaneously. With a judicious selection of the transformation matrix U, this is always possible if the following conditions are satisfied: one, the matrix I is positive definite and invertible, and two, the I and K matrices are real and symmetric. If these conditions are satisfied, then there exists an orthogonal matrix U that can be used to uncouple or diagonalize the system. This is true for the system of interest of this report but the proof is beyond the scope of this paper [17]. Also, note that it is sometimes possible to diagonalize systems where the coefficient matrices are not real and symmetric; i.e., there may

20

exist a transformation matrix U that will diagonalize the system but there is not necessary one! In this case, one would use the inverse of the transformation matrix U instead of the transpose.

The next question one should ask is how is the transformation matrix U determined? The transformation matrix U is just the eigenvectors of the system of interest. Thus, one would pre-multiply through equation 22 by the inverse of matrix I (which is where the requirement for matrix I being invertible comes from) and form a new coefficient matrix for the vector η represented by a new matrix, A.

$$\{\ddot{\eta}\} + [A]\{\eta\} = \{0\} \tag{27}$$

where $$[A] = [I]^{-1} [K]$$

So the eigenvectors of the matrix A form the transformation or modal matrix U that were used in equation 23 to map the original coordinates, η, into the new or generalized coordinates, q.

Once this mathematical technique is used, the resulting system of equations are uncoupled and lend themselves to solution by any of the various common means of solving ordinary differential equations such as Laplace or Fourier methods. Applying this modal method to equation 22 results in equations of the form of equation 26 with the explicit equations being:

$$\begin{bmatrix} m_1 & 0 \\ 0 & m_2 \end{bmatrix} \begin{bmatrix} \ddot{q}_1 \\ \ddot{q}_2 \end{bmatrix} + \begin{bmatrix} k_1 & 0 \\ 0 & k_2 \end{bmatrix} \begin{bmatrix} q_1 \\ q_2 \end{bmatrix} = \begin{bmatrix} \mp z_1 \\ \mp z_2 \end{bmatrix} \tag{28}$$

One solution set to these equations is for $k_1 > 0$ and $k_2 > 0$:

$$q_1(t) = E_{11} \cos w_1 t + E_{12} \sin w_1 t \mp \frac{z_1}{k_1} \tag{29a}$$

$$q_2(t) = E_{21} \cos w_2 t + E_{22} \sin w_2 t \mp \frac{z_2}{k_2} \tag{29b}$$

or, if $k_1 < 0$ and $k_2 < 0$ then:

$$q_1(t) = E_{11} \cosh w_1 t + E_{12} \sinh w_1 t \mp \frac{z_1}{k_1} \tag{30a}$$

21

$$q_2(t) = E_{21} \cosh w_2 t + E_{22} \sinh w_2 t \mp \frac{z_2}{k_2} \qquad (30b)$$

where the trigonometric or hyperbolic functions comprise the homogeneous solution while the last terms are the particular solution to equation 28. Both solution sets need to be considered since the sign of the k_i term in each equation drives which equation is used. For example, if k_1 is negative, then the correct solution for $q_1(t)$ would be equation 30a. It is entirely possible that for the same system, k_2 is positive and thus the correct solution for $q_2(t)$ would be equation 29b. Therefore, these two independent solutions would comprise the solution set to equation 28, the solution with respect to the general or transformed coordinates. Also, since the k_i terms in equation 28 are functions of the original K matrix via the modal mapping process, and since the original K matrix is case dependent, i.e., the sign and magnitude of the K_{ij} terms can vary among the four cases or regimes of motion, the character of the solution set for equation 28 can vary whenever the cases change.

Now the k_i terms govern whether the form of the solution is trigonometric or hyperbolic, but these stiffness parameters are valid only in the generalized coordinate system. To understand physically when the solutions change character, the value of the k_i terms at the critical point ($k_i = 0$) must be understood within the context of the original coordinate system. As given by equation 26

$$[k] = [U]^T [K][U] \qquad (31)$$

or explicitly

$$k_1 = u_{11}^2 K_{11} + u_{11} u_{21} (K_{12} + K_{21}) + u_{21}^2 K_{22} \qquad (32a)$$

$$k_2 = u_{12}^2 K_{11} + u_{12} u_{22} (K_{12} + K_{21}) + u_{22}^2 K_{22} \qquad (32b)$$

Assuming that the two original springs are placed symmetrically, have the same stiffness and substituting in the explicit expressions for K_{ij} terms from page 18, then at $k_1 = 0$ and $k_2 = 0$ expressions can be derived to determine the values at which the original spring stiffness causes a change in the character of the solution.

$$K_1 = \frac{A + B\left[2 + \left(\frac{u_{21}}{u_{11}}\right)^2\right]}{(b_2 + l_1)(l_1 + l_2)\left[1 - 2\left(\frac{u_{21}}{u_{11}}\right) + \left(\frac{u_{21}}{u_{11}}\right)^2\right]} \qquad (33a)$$

$$K_2 = \frac{A + B\left[2 + \left(\frac{u_{22}}{u_{12}}\right)^2\right]}{(b_2 + l_2)(l_1 + l_2)\left[1 - 2\left(\frac{u_{22}}{u_{12}}\right) + \left(\frac{u_{22}}{u_{12}}\right)^2\right]} \qquad (33b)$$

where $\qquad A = m_1 a_1 g \quad$ and $\quad B = m_2 a_1 g$

Thus, the values of the original stiffness terms at which the solution changes character are functions of the eigenvectors of the system which change as the original stiffness terms change in value. This means that for a specific stiffness, there is a corresponding critical value at which the solution changes character. If the original stiffness changes, then the critical value will change also! The specifics of this as it relates to this problem will be discussed in section 4.

The w_1 and w_2 terms in equations 29 and 30 are just the eigenvalues of the system represented by equation 28 and are determined by equations 34a and 34b.

$$w_1 = \sqrt{\frac{|k_1|}{m_1}} \qquad (34a)$$

$$w_2 = \sqrt{\frac{|k_2|}{m_2}} \qquad (34b)$$

Since the m_i terms represent a physical quantity, the mass, they are always positive; therefore, the sign of the k_i terms determines whether the solution set to equation 28, as outlined in equations 29 or 30, contain trigonometric or hyperbolic functions.

The E_{ii} coefficients in equations 29 and 30 are determined from the transformed initial conditions, i.e., the initial velocities and displacements of each block respectively. Since an analytic solution of equation 22 is known only in the generalized coordinate system or space, it is necessary to map the original initial conditions to this space also. This is accomplished by the use of equations 35a and 35b.

$$\{q(0)\} = [m][U]^T[I]\{\eta(0)\}$$ (35a)

$$\{\dot{q}(0)\} = [m][U]^T[I]\{\dot{\eta}(0)\}$$ (35b)

where $[m] = [U]^T[I][U]$ from equation 26, matrix U is the modal matrix, matrix I is the original inertia matrix for the $\ddot{\eta}$ vector, and the η and $\dot{\eta}$ vectors are the initial coordinates for the displacements and velocities, respectively. In explicit form, equations 35a and 35b are:

$$\begin{bmatrix} q_1(0) \\ q_2(0) \end{bmatrix} = \begin{bmatrix} m_1 & 0 \\ 0 & m_2 \end{bmatrix}\begin{bmatrix} u_{11} & u_{21} \\ u_{12} & u_{22} \end{bmatrix}\begin{bmatrix} i_{11} & i_{12} \\ i_{21} & i_{22} \end{bmatrix}\begin{bmatrix} \eta_1(0) \\ \eta_2(0) \end{bmatrix}$$ (36a)

$$\begin{bmatrix} \dot{q}_1(0) \\ \dot{q}_2(0) \end{bmatrix} = \begin{bmatrix} m_1 & 0 \\ 0 & m_2 \end{bmatrix}\begin{bmatrix} u_{11} & u_{21} \\ u_{12} & u_{22} \end{bmatrix}\begin{bmatrix} i_{11} & i_{12} \\ i_{21} & i_{22} \end{bmatrix}\begin{bmatrix} \dot{\eta}_1(0) \\ \dot{\eta}_2(0) \end{bmatrix}$$ (36b)

Once the generalized initial conditions are determined via equations 36a and 36b, it is relatively simple to rearrange equations 23 or 24 to solve for the E_{ii} coefficients. The rearranged equations 23 or 24 now become at $t = 0$,

$$E_{11} = q_1(0) \pm \frac{z_1}{k_1}$$ (37a)

$$E_{21} = q_2(0) \pm \frac{z_2}{k_2}$$ (37b)

and coefficients E_{12} and E_{22} are found by taking the derivative of equations 23 or 24 and then rearranging the terms to get,

24

$$E_{12} = \frac{\dot{q}_1(0)}{w_1} \tag{37c}$$

$$E_{22} = \frac{\dot{q}_2(0)}{w_2} \tag{37d}$$

Thus, equations 29 and 30 can now be evaluated to provide the solution to the system equation 28.

These analytic solutions, $q_1(t)$ and $q_2(t)$, are valid only in the generalized coordinate system since they were only possible to obtain in that space and must be converted back to the original coordinate system to produce the proper displacements, velocities, and more importantly, the physical understanding of the dynamics of the problem. Once the generalized solutions are obtained as a function of time they are transformed back to the original coordinate system by equations 38a and 38b.

$$\theta(t) = u_{11}q_1(t) + u_{12}q_2(t) \tag{38a}$$

$$\alpha(t) = u_{21}q_1(t) + u_{22}q_2(t) \tag{38b}$$

where, as before, the u_{ii} coefficients are merely the elements of the modal matrix U,

i.e.,
$$[U] = \begin{bmatrix} u_{11} & u_{12} \\ u_{21} & u_{22} \end{bmatrix}$$

Computationally, this process is done at each time step to produce the correct motion and time history of the rocking blocks. The complete time history of the rocking blocks then becomes the aggregate of the motion as evaluated at each discrete time step. However, one must account for the discontinuities that occur at each impact, which is represented mathematically as the transition from one set of equations of motion with their corresponding analytic solutions to the correct or new equations of motion with their corresponding solutions, by evaluating the local time history and generating new initial conditions for the next regime of motion. As with the SDOF system, the assumption was made that by using conservation of moment of momentum, a relationship could be derived relating the new initial conditions to the previous initial conditions to account for the discontinuity at impact. This procedure, as discussed in section 2 of this report, allows the derivation of equations that account

25

for the energy dissipated during the transition from one regime of motion to the next. However, instead of one equation, as was the case for the SDOF system, this method provides two equations, as is to be expected for a two DOF system. As before, these equations are a function of the geometry of the system and in addition, they are functions of the mass and impact velocities. In effect, these equations bridge the discontinuities between the four regimes of motion and allow the calculation of the new angular velocities required as two of the four initial conditions for the next regime of motion.

One important consideration for a 2DOF system is how to apply conservation of angular momentum to this system. As mentioned before, two independent transition equations are required to solve this problem in closed form, but there are three possible applications of this principle: conservation of system angular momentum or conservation of the angular momentum of each block. For this particular system, conservation of angular momentum holds true for the system and the top block only! The angular momentum of the bottom block is not conserved. The proof resides in the appendix. The transition equations, which are rather complex and involved, corresponding to this specific model of a two DOF system are presented below and are mathematically equivalent to the equations first derived by Psycharis [13].

For θ - transition from case 1 to case 4 or case 3 to case 2

$$\dot{\theta}_f = c_1 \dot{\theta}_i \tag{39a}$$

$$\dot{\alpha}_f = \dot{\alpha}_i + d_1 \dot{\theta}_i \tag{39b}$$

where
$$c_1 = \frac{j_2 j_3 - j_1 j_4}{j_3 j_3 - j_1 j_5} \qquad d_1 = \frac{j_2}{j_1} - \frac{j_3}{j_1} c_1$$

and
$$j_1 = I_{B2C2} + m_2 (a_2{}^2 + b_2{}^2)$$

$$j_2 = m_2 [b_2 (b_1 - l_1) + (2 a_1 h_2)]$$

$$j_3 = -m_2 [b_2 (b_1 + l_2) - (2 a_1 h_2)]$$

$$j_4 = I_{B1C1} + m_1 (h_1{}^2 - b_1{}^2) + m_2 [(2 a_1)^2 - (h_1 - l_2)(b_1 + l_2)]$$

$$j_5 = I_{B1C1} + m_1 (a_1{}^2 + b_1{}^2) + m_2 [(2 a_1)^2 + (b_1 + l_2)^2]$$

26

For θ - transition from case 4 to case 1 or case 2 to case 3, which is physically the reverse of the previous transition, the form of the transition equations are the same, but the j_i expressions are slightly different as shown below.

$$j_1 = I_{B2C2} + m_2 (a_2^2 + b_2^2) \tag{40a}$$

$$j_2 = -m_2 [b_2 (b_1 + l_2) - (2 a_1 h_2)] \tag{40b}$$

$$j_3 = m_2 [b_2 (b_1 - l_2) + (2 a_1 h_2)] \tag{40c}$$

$$j_4 = I_{B1C1} + m_1 (h_1^2 + b_1^2) + m_2 [(2 a_1)^2 - (b_1 - l_2)(b_1 + l_2)] \tag{40d}$$

$$j_5 = I_{B1C1} + m_1 (a_1^2 + b_1^2) + m_2 [(2 a_1)^2 + (b_1 - l_2)^2] \tag{40e}$$

For α - transition from case 1 to 2 or case 3 to 4

$$\dot{\theta}_f = (c_2 + \lambda d_2) \dot{\theta}_i \tag{41a}$$

$$\dot{\alpha}_f = (c_3 + \lambda d_3) \dot{\alpha}_i \tag{41b}$$

where $\quad c_2 = \dfrac{j_2 j_4 - j_1 j_7}{j_2 j_2 - j_1 j_5} \quad d_2 = \dfrac{j_2 j_3 - j_1 j_6}{j_2 j_2 - j_1 j_5} \quad \lambda = \dfrac{\dot{\alpha}_i}{\dot{\theta}_i}$

and $\quad c_3 = \dfrac{j_4 j_5 - j_2 j_7}{j_1 j_5 - j_2 j_2} \quad d_3 = \dfrac{j_3 j_5 - j_2 j_6}{j_1 j_5 - j_2 j_2}$

and $\quad j_1 = I_{B2C2} + m_2 (a_2^2 + b_2^2)$

$j_2 = -m_2 [b_2 (b_1 + l_2) - (2 a_1 h_2)]$

$j_3 = I_{B2C2} + m_2 (a_2^2 + b_2^2) - 2 m_2 b_2^2$

$j_4 = -m_2 [b_2 (b_1 - l_2) - (2 a_1 h_2)]$

$j_5 = I_{B1C1} + m_1 (a_1^2 + b_1^2) + m_2 [(2 a_1)^2 + (b_1 + l_2)^2]$

$j_6 = m_2 [2 b_2^2 + 2 a_1 a_2 + b_2 (b_1 - l_2)]$

$j_7 = I_{B1C1} + m_1 (a_1^2 + b_1^2) + m_2 [(b_1 - l_2)^2 + (2 a_1)^2 + 2 b_2(b_1 - l_2)]$

27

For α - transition from case 2 to case 1 or case 4 to case 3 , which is physically the reverse of the previous transition, the form of the transition equations are the same, but the j_i expressions are slightly different as shown below in equations 42.

$$j_1 = I_{B2C2} + m_2 (a_2{}^2 + b_2{}^2) \tag{42a}$$

$$j_2 = m_2 [b_2 (b_1 - l_2) + (2 a_1 h_2)] \tag{42b}$$

$$j_3 = I_{B2C2} + m_2 (a_2{}^2 + b_2{}^2) - 2 m_2 b_2{}^2 \tag{42c}$$

$$j_4 = m_2 [b_2 (b_1 + l_2) + (2 a_1 h_2)] \tag{42d}$$

$$j_5 = I_{B1C1} + m_1 (a_1{}^2 + b_1{}^2) + m_2 [(2 a_1)^2 + (b_1 - l_2)^2] \tag{42e}$$

$$j_6 = m_2 [2 b_2{}^2 + 2 a_1 a_2 - b_2 (b_1 + l_2)] \tag{42f}$$

$$j_7 = I_{B1C1} + m_1 (a_1{}^2 + b_1{}^2) + m_2 [(b_1 + l_2)^2 + (2 a_1)^2 - 2 b_2 (b_1 + l_2)] \tag{42g}$$

It is also possible to derive transition equations using conservation of energy principles, but there are drawbacks to using such a method. Though the derivation of the expressions relating the pre-impact angular velocities to the post-impact angular velocities is rather straightforward and somewhat less tedious, the final expressions are more complex and less tractable. The final expressions are nonlinear because of the velocity squared terms, the velocity coupled terms, and the trigonometric functions of the displacement angles. Ignoring these difficulties still requires one to arbitrarily select a "coefficient of restitution" term to account for the energy loss due to impact. If the selected value for this term is too large in magnitude, then physically this is equivalent to adding energy to the system which then undergoes larger and larger oscillations until the system topples. Using the conservation of angular momentum method prevents this by determining the upper theoretical value for the coefficient of restitution term from geometrical considerations as stated before. Note that it is still possible for the system under consideration to topple under the appropriate conditions; but if that phenomenon occurs, then it is a function of the initial conditions and the geometry of the problem, not due to some lack of accountability of energy dissipation during transition.

Another significant consideration with transition involving the computational aspect is how to determine which state the system lies in when one of the two coordinates is exactly at the transition point, i.e., $\theta = 0$ or $\alpha = \theta$. Mathematically, the equations of motion are undefined at these points, which is why the transition equations are needed; but it is still necessary to be able to determine which regime of motion the system will enter after going through transition. The reason for this is that it is necessary to calculate the correct post-impact initial conditions, i.e., the correct

values of θ, α, $\dot{\theta}$ and $\dot{\alpha}$. Also, it is important to realize that though this report considers the four main regimes of motion, as mentioned previously, it is possible for the system to rock as a SDOF system (both blocks rock in tandem), or it is possible that only the top block will rock. The reasons for not discussing these cases in depth here has been explained previously but the possibility of these cases occurring must still be accounted for computationally to obtain the correct system response.

After each time step calculation, the case or regime of motion was determined by the values associated with the θ and α parameters. Transition occurs when the current case differs from the previous case. At this point, since the pre-impact and post-impact cases are known, the transition equations are used to recalculate the current time step's angular velocities for the two new initial conditions for the post-impact case. The displacement angle of the block undergoing transition was set equal to its transition point, i.e., $\theta = 0$ for a bottom block impact or $\alpha = \theta$ for a top block impact. The other displacement angle retains its previous value; thus, there are now four new initial conditions for the post-impact case. These new initial conditions are mapped to a set of generalized initial conditions and the next local solution for this time step is determined. When one or both blocks are at a transition point, then the angular velocities are examined to determine the post-impact case or regime. Note that when the post-impact case is determined by the values of the angular velocities, it is the angular velocities as determined from the transition equations that are used.

It is possible that the velocities can change sign and by orders of magnitude during transition. The change of sign requires that for computational reasons one must consider the relative velocities of the blocks to determine whether they will rock in tandem or separate. In other words, there are some velocities as calculated by the transition equations that are physically impossible to attain in order to maintain the physical integrity of the blocks. The process is complex and as an aid to understanding the decision algorithm is provided in Figures 5 through 7. For completeness, cases 5, 6 and 7 were added to the four main cases, as shown previously in Figure 4. Case 5 is the case where both blocks are rocking together, or mathematically, where $\alpha = \theta$ always. Once this condition occurs, the system will remain in this state at least until the bottom block impacts. Then it is possible for the other cases to occur. Case 6 corresponds to the situation where the bottom block is motionless and the top block is rocking. This is analogous to the SDOF system or the single rocking block problem. Case 7 is simply the case where all system motion has ceased and is included as a computational aid.

Thus, it is possible to calculate and model the motion of a 2DOF system representing a turreted vehicle; however, the primary motivation of this method is the calculation and prediction of the acceleration levels, as a function of the gross motion of the vehicle, at any point within the structure. The solution of equations 17 through 20 in terms of θ and α allows the calculation of acceleration levels as a function of these two parameters and the geometry of the system under scrutiny. The method and equations are presented next.

29

Since it is necessary to derive the acceleration equations to determine the proper expression for the equations of motion, these equations are just presented below. See appendix A, a sample calculation, for more detail.

CASE 1 --> $\theta > 0$, $\alpha > 0$

$$\underset{\sim}{a}(p_1/\varepsilon) = (x_1\ddot{\theta} - y_1\dot{\theta}^2)\underset{\sim}{j} - (y_1\ddot{\theta} + x_1\dot{\theta}^2)\underset{\sim}{i} \tag{43a}$$

$$\underset{\sim}{a}(p_2/\varepsilon) = ((b_1 - l_1)\ddot{\theta} - 2a_1\dot{\theta}^2)\underset{\sim}{j} - ((b_1 - l_1)\dot{\theta}^2 + 2a_1\ddot{\theta})\underset{\sim}{i}$$
$$+ (x_2\ddot{\alpha} - y_2\dot{\alpha}^2)\underset{\sim}{v} - (x_2\dot{\alpha}^2 + y_2\ddot{\alpha})\underset{\sim}{u} \tag{43b}$$

CASE 2 --> $\theta > 0$, $\alpha \leq 0$

$$\underset{\sim}{a}(p_1/\varepsilon) = (x_1\ddot{\theta} - y_1\dot{\theta}^2)\underset{\sim}{j} - (y_1\ddot{\theta} + x_1\dot{\theta}^2)\underset{\sim}{i} \tag{44a}$$

$$\underset{\sim}{a}(p_2/\varepsilon) = ((b_1 + l_2)\ddot{\theta} - 2a_1\dot{\theta}^2)\underset{\sim}{j} - ((b_1 + l_2)\dot{\theta}^2 + 2a_1\ddot{\theta})\underset{\sim}{i}$$
$$+ ((2b_2 - x_2)\ddot{\alpha} - y_2\dot{\alpha}^2)\underset{\sim}{v} + ((2b_2 - x_2)\dot{\alpha}^2 + y_2\ddot{\alpha})\underset{\sim}{u} \tag{44b}$$

CASE 3 --> $\theta \leq 0$, $\alpha \leq 0$

$$\underset{\sim}{a}(p_1/\varepsilon) = ((2b_1 - x_1)\ddot{\theta} - y_1\dot{\theta}^2)\underset{\sim}{j} + ((2b_1 - x_1)\dot{\theta}^2 + y_1\ddot{\theta})\underset{\sim}{i} \tag{45a}$$

$$\underset{\sim}{a}(p_2/\varepsilon) = ((b_1 - l_2)\ddot{\theta} - 2a_1\dot{\theta}^2)\underset{\sim}{j} - ((b_1 - l_2)\dot{\theta}^2 + 2a_1\ddot{\theta})\underset{\sim}{i}$$
$$+ ((2b_2 - x_2)\ddot{\alpha} - y_2\dot{\alpha}^2)\underset{\sim}{v} + ((2b_2 - x_2)\dot{\alpha}^2 + y_2\ddot{\alpha})\underset{\sim}{u} \tag{45b}$$

CASE 4 --> $\theta \leq 0$, $\alpha > 0$

$$\underset{\sim}{a}(p_1/\varepsilon) = ((2b_1 - x_1)\ddot{\theta} - y_1\dot{\theta}^2)\underset{\sim}{j} + ((2b_1 - x_1)\dot{\theta}^2 + y_1\ddot{\theta})\underset{\sim}{i} \tag{46a}$$

$$\underset{\sim}{a}(p_2/\varepsilon) = ((b_1 + l_1)\ddot{\theta} - 2a_1\dot{\theta}^2)\underset{\sim}{j} + ((b_1 + l_1)\dot{\theta}^2 + 2a_1\ddot{\theta})\underset{\sim}{i}$$
$$+ (x_2\ddot{\alpha} - y_2\dot{\alpha}^2)\underset{\sim}{v} - (x_2\dot{\alpha}^2 + y_2\ddot{\alpha})\underset{\sim}{u} \tag{46b}$$

30

where points p_1 and p_2 are the arbitrary points in bodies B_1 and B_2 where the acceleration levels need to be determined. Parameters x_1, y_1 and x_2, y_2 are the coordinates of points p_1 and p_2 with respect to the inertial reference frame ε. The vectors $\underline{i}$, $\underline{j}$ $\underline{\mu}$ and $\underline{v}$ are unit vectors with the following relationships to the inertial reference frame, $\varepsilon\,(X,\,Y)$.

CASE 1 --> $\theta \geq 0$, $\alpha \geq \theta$

$$\underline{i} = \cos\theta \underline{X} + \sin\theta \underline{Y} \qquad \underline{j} = \cos\theta \underline{Y} - \sin\theta \underline{X}$$

$$\underline{\mu} = \cos\alpha \underline{X} + \sin\alpha \underline{Y} \qquad \underline{v} = \cos\alpha \underline{Y} - \sin\alpha \underline{X}$$

CASE 2 --> $\theta \geq 0$, $\alpha \leq \theta$

$$\underline{i} = \cos\theta \underline{X} + \sin\theta \underline{Y} \qquad \underline{j} = \cos\theta \underline{Y} - \sin\theta \underline{X}$$

$$\underline{\mu} = \cos\alpha \underline{X} - \sin\alpha \underline{Y} \qquad \underline{v} = \cos\alpha \underline{Y} + \sin\alpha \underline{X}$$

CASE 3 --> $\theta \leq 0$, $\alpha \leq \theta$

$$\underline{i} = \cos\theta \underline{X} - \sin\theta \underline{Y} \qquad \underline{j} = \cos\theta \underline{Y} - \sin\theta \underline{X}$$

$$\underline{\mu} = \cos\alpha \underline{X} - \sin\alpha \underline{Y} \qquad \underline{v} = \cos\alpha \underline{Y} + \sin\alpha \underline{X}$$

CASE 4 --> $\theta \leq 0$, $\alpha \geq \theta$

$$\underline{i} = \cos\theta \underline{X} - \sin\theta \underline{Y} \qquad \underline{j} = \cos\theta \underline{Y} - \sin\theta \underline{X}$$

$$\underline{\mu} = \cos\alpha \underline{X} + \sin\alpha \underline{Y} \qquad \underline{v} = \cos\alpha \underline{Y} - \sin\alpha \underline{X}$$

Modal analysis enables the decoupling of the system equations and the determination of analytic solutions as functions of the system parameters in the form of coefficient matrices. This allows the conduct of parameter studies by adjusting the coefficient matrices, and, in the case of the stiffness matrix, possibly changing the form of the solution to understand the effect of varying spring stiffness. The implications and results are presented in the next section.

31
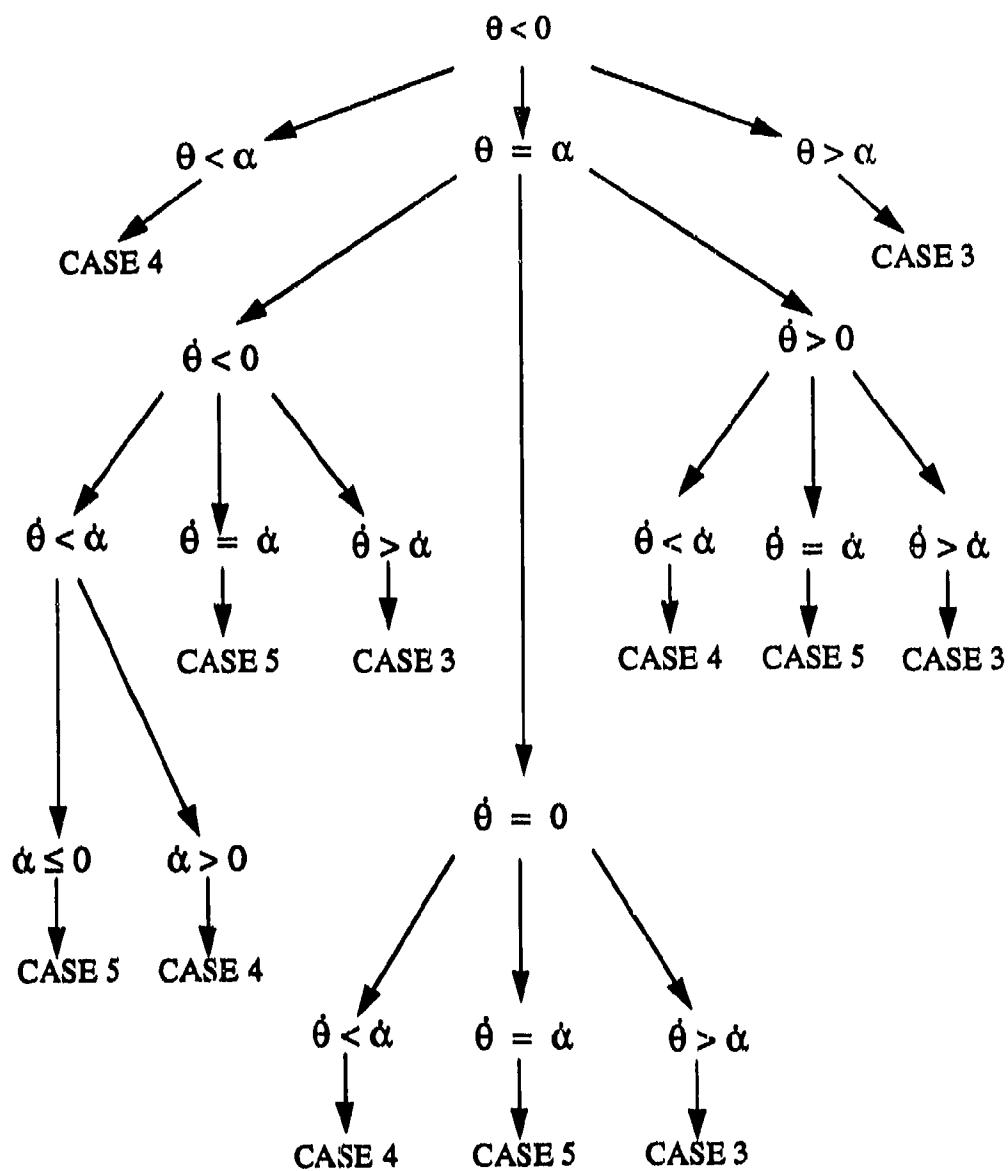
FIGURE 5 - Decision Tree for $\theta < 0$

32

θ = 0

θ < α   θ > α

$\dot\theta < 0$ $\dot\theta = 0$ $\dot\theta > 0$ $\dot\theta < 0$ $\dot\theta = 0$ $\dot\theta > 0$

CASE 4   CASE 6   CASE 1   CASE 3   CASE 6   CASE 2

θ = α

$\dot\theta < 0$ $\dot\theta > 0$

$\ddot\theta < \alpha$ $\ddot\theta = \alpha$ $\ddot\theta > \alpha$ $\ddot\theta < \alpha$ $\ddot\theta = \alpha$ $\ddot\theta > \alpha$

CASE 5   CASE 5   CASE 3   CASE 1   CASE 5

$\dddot\alpha < 0$ $\dddot\alpha \geq 0$

CASE 2   CASE 5

$\dot\theta = 0$

$\ddot\theta < \alpha$ $\ddot\theta = \alpha$ $\ddot\theta > \alpha$

CASE 6   CASE 7   CASE 6
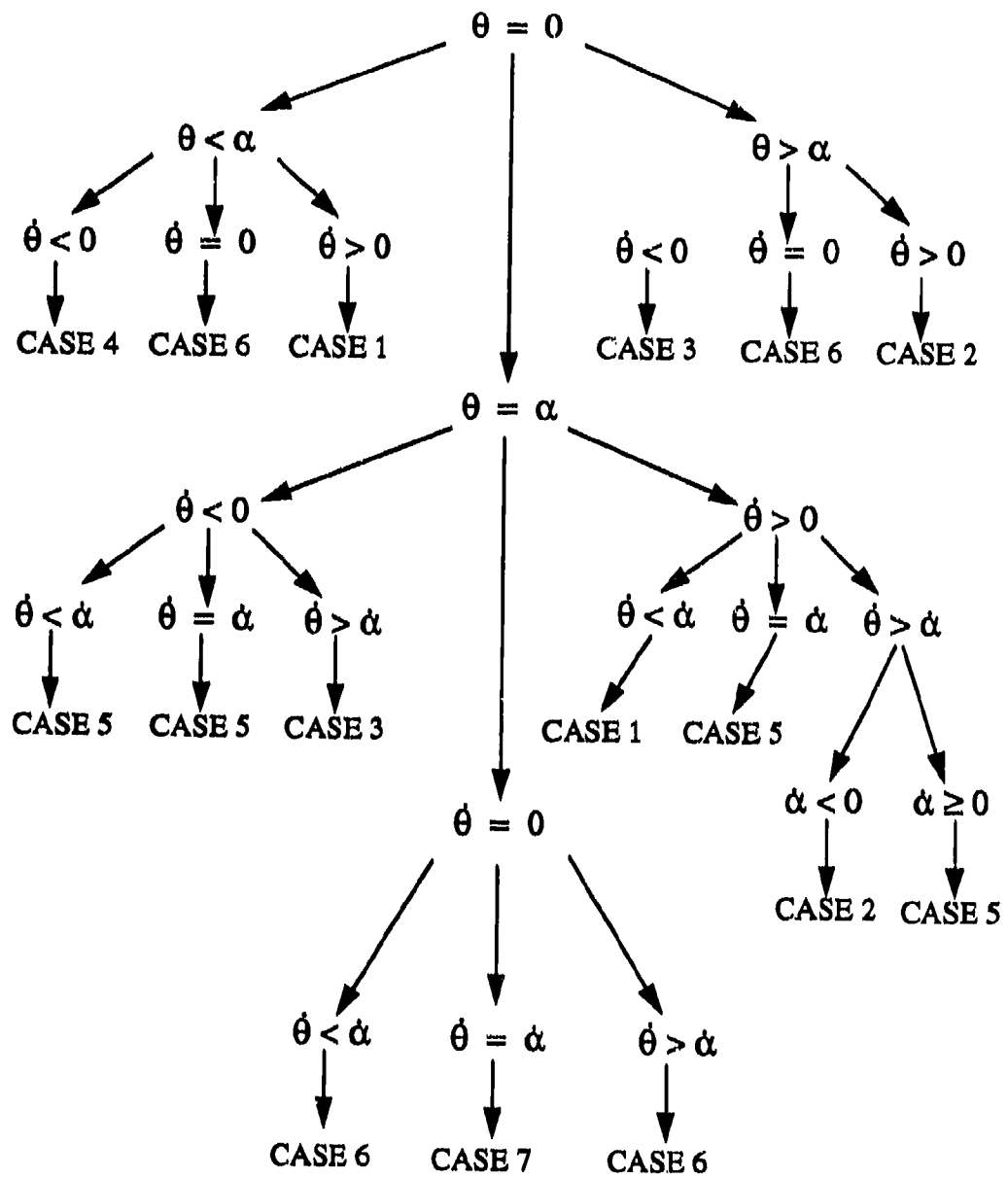
FIGURE 6 - Decision Tree for θ = 0

33
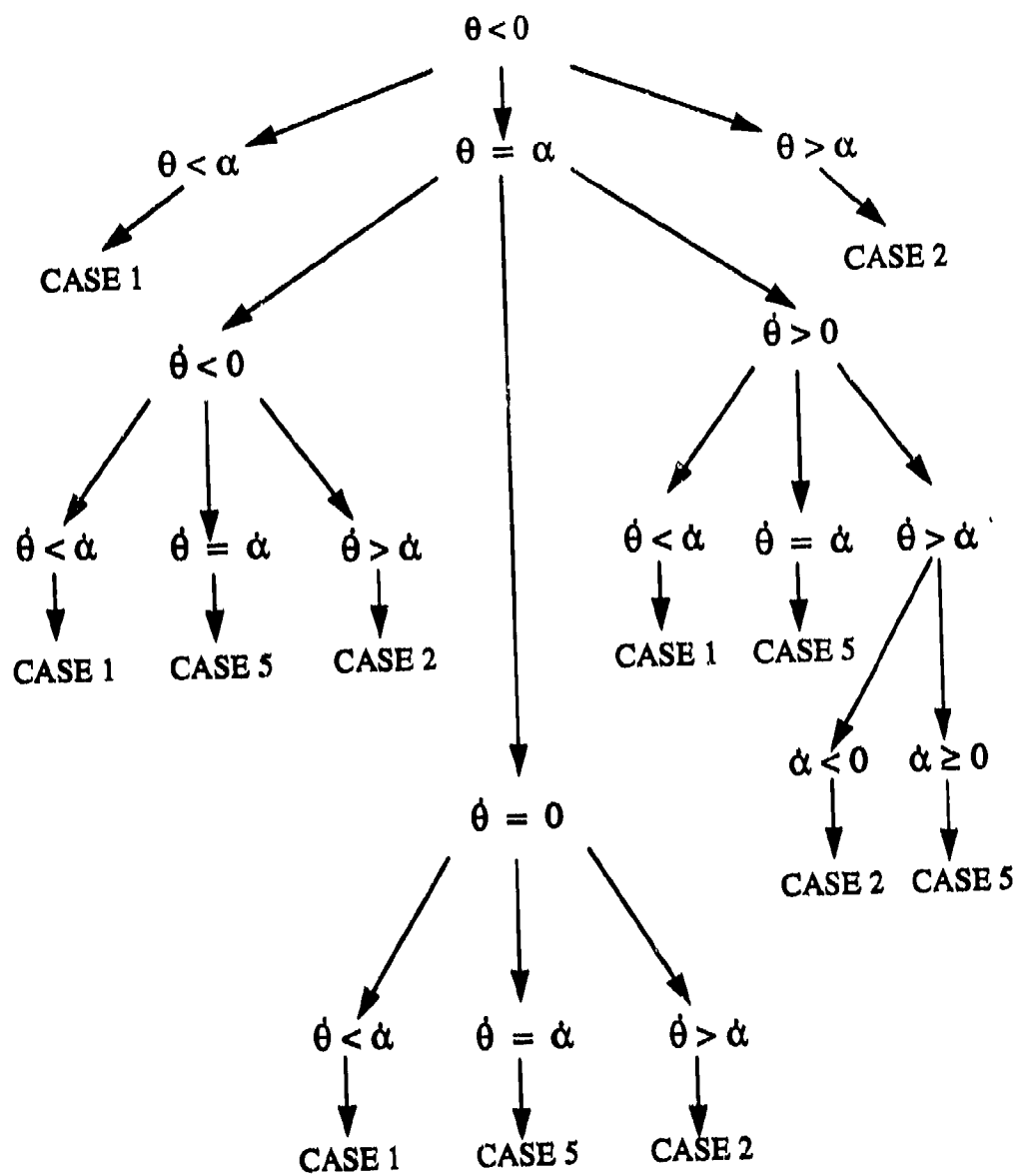
FIGURE 7 - Decision Tree for $\theta > 0$

34

4. RESULTS

The analytical solutions presented in section 3 were incorporated within two computer programs (FORTRAN 77) so that parametric studies of the effect of various values of the inertia and stiffness coefficient matrices could be determined. The first program simulated the single rocking block (SDOF) system while the second program simulated the more complex stacked rocking block (2DOF) system. The SDOF code was run on a SUN 3/50 workstation at 32-bit precision and the 2DOF code was run on a CRAY XMP/416 supercomputer at 64-bit single precision with a time step of 0.001 sec. The codes were also run with time steps of 0.0001 sec with no significant differences in the values obtained. All the results presented here were generated using time steps of 0.001 sec.

For the SDOF system, the block was considered to be homogeneous with a square base, $b_1 = 4\,ft$ and half-height of $a_1 = 4\,ft$. Thus, this block was cubic and had dimensions of $8x8x8\,ft$. A density of $145\,lbs/ft^3$ was assumed, representing concrete. The block was displaced 0.40 radians in the positive direction with no initial angular velocity and allowed to rotate in free vibration. Six values of the K_1 term were compared for their effect on the system response. The results are presented in Figure 8.

The trend shown in Figure 8 is rather evident; as the K_1 term increases in magnitude, i.e., the system becomes "stiffer," the block impacts sooner (*at $t = 0.15$ sec for $K = 5,000,000$ lbs/ft versus $t = 0.63$ sec for $K = 0$*) and the succeeding amplitudes of each peak are greater for larger values of K. This is to be expected since this represents typical behavior for SDOF systems modeled as simple harmonic oscillators. Holding the initial displacement constant while increasing the stiffness of the spring constant is equivalent to adding energy to the system in the form of potential energy of the spring. Thus, the stiffer systems have more energy and it is expected that they would impact sooner and harder than the more flexible systems. This is also why the post-impact response is more energetic for the stiffer systems since the energy dissipated during transition percentage-wise is the same regardless of the stiffness. Note that this system is not a viscously damped harmonic oscillator, though the governing equations of both are the same, since the physical model of the single block includes energy dissipation within the code to account for the change in the pole of rotation during transition. An undamped harmonic oscillator would vibrate indefinitely with no energy loss while this system eventually damps out due to the instantaneous angular velocity reduction at impact from the transition equation, which is a function of the system geometry. Note that for this specific example from

35

TIME HISTORY OF SINGLE BLOCK

Legend:
— K=0 lbs/ft
·· K=50000 lbs/ft
··· K=150,000 lbs/ft
—· K=300,000 lbs/ft
—· K=1,000,000 lbs/ft
···· K=5,000,000 lbs/ft
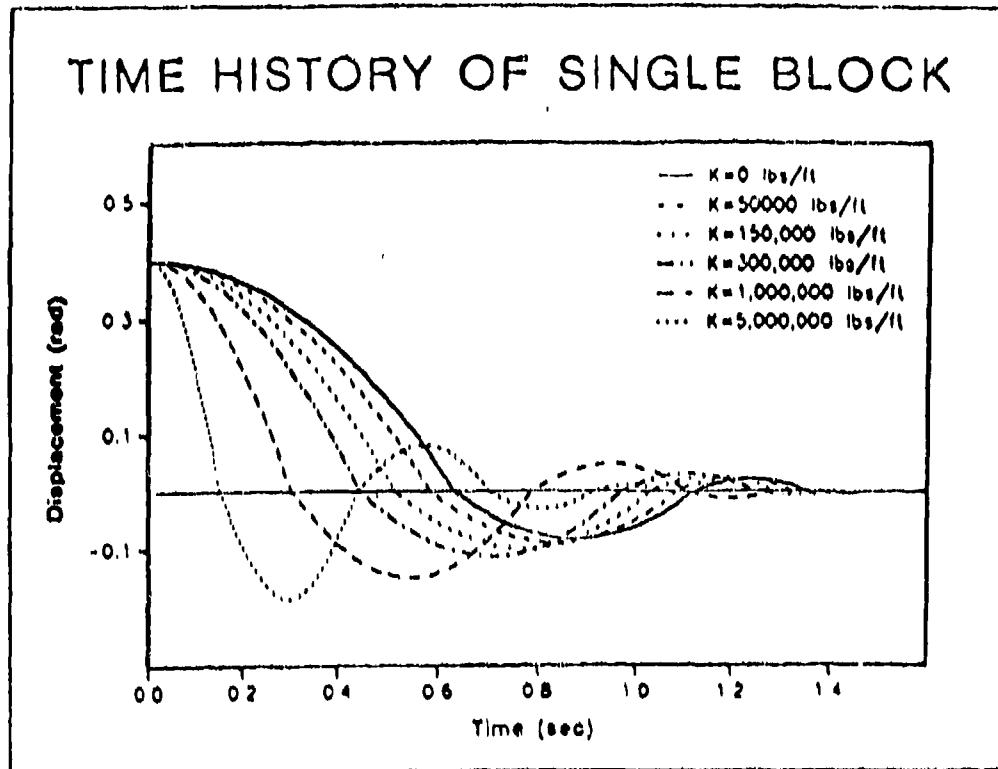
FIGURE 8 - Free Vibration of Single Block as a Function of K

equation 11, $C = 0.25$ so that the reduction in velocity at each impact is *75%*, while using equation 11, the energy loss is roughly *94%* ! It is important to note that the spring, which can be thought of as an energy storage element which neither creates nor destroys energy, has no effect on the transition of the system in terms of energy. The most significant aspect of this example is that even though the value of K increases by orders of magnitude, the system response varies very slowly until the difference in magnitude is around an order of 5. Thus, it appears that the system response, though a function of K, is a relatively weak function.

For the parameters chosen for this problem, and using equations 4 and 5, the values at which the solution changes character was determined and is presented in Table 1. Note that $K_{cr} = 149,408.0$ from equation 7. Thus, it is evident that the character of the solution changes when the stiffness of the spring was set at *150,000 lbs/ft;* but it is interesting to note in Figure 8 that the response of the block did not change significantly. It is somewhat surprising from a mathematical viewpoint that when the character of the solution changes, the system response is relatively benign. This is more evidence that the system response is a weak function of the stiffness.

36

TABLE 1 - SDOF Character of Solution at Various Stiffness

K (lbs/ft)	A (1/sec)
0	-12.0750
50,000	-8.0341
150,000	0.0478
300,000	12.1707
1,000,000	68.7440
5,000,000	392.0198

For the 2DOF system, both blocks were considered to be homogeneous, stacked symmetrically, and to have square bases such that $b_1=4\,ft$ and $b_2=2\,ft$. The height of the bottom block was $2a_1=8\,ft$ and the top block was $2a_2=4\,ft$, so both blocks were cubic in nature with the dimensions of the bottom block being $8x8x8\,ft$ while the top block was $4x4x4\,ft$.

The first parametric study was to consider how the system response varied with the ratio of the densities of the blocks. The density of the top block was kept constant at $\rho_2 = 145\ lbs/ft^3$ as the density of the bottom block, ρ_1, varied in multiples of the top block's density represented as the ratio $P = \rho_1/\rho_2$. The bottom block was given an initial displacement of $\theta_0 - 0.4$ rads with no initial angular velocity, while the top block was initially displaced at $\alpha_0 - 0.5$ rads with no initial velocity. The value associated with the parameter K was kept constant at zero. The response of the top block is presented in Figure 9 and the response of the bottom block is presented in Figure 10.

Considering the motion history of the top block first, it is evident that as the mass of the bottom block increases relative to the top block, i.e., an increasing P ratio, that the top block's motion becomes less muted or gradual until impact of the bottom block at which time the additional mass associated with the top block relative to the bottom block, i.e., a smaller P ratio, allows for a greater response of the top block in terms of amplitude and duration after impact. Since conservation of angular momentum is the principle that bridges the two regimes of motion, this type of response is expected and reasonable. Also, note that a comparison of Figures 9 and 10 show that the sudden change in the slope of the P curves in Figure 9 correspond to impacts by the bottom block. This is explained by the instantaneous velocity reductions that occur for the top block during impact of the bottom block. There are certain conditions that cause the top block to increase its displacement beyond the initial displacement due to the interaction of the bottom block as shown in Figure 9. As the higher P ratio shows, this phenomenon occurs when the mass of the top block is relatively less than the bottom block's mass. It is even possible under some conditions for the top block to topple due to its coupling with the bottom block, whereas this behavior is not seen with the SDOF system. This will be discussed after considering the motion of the bottom block.

37
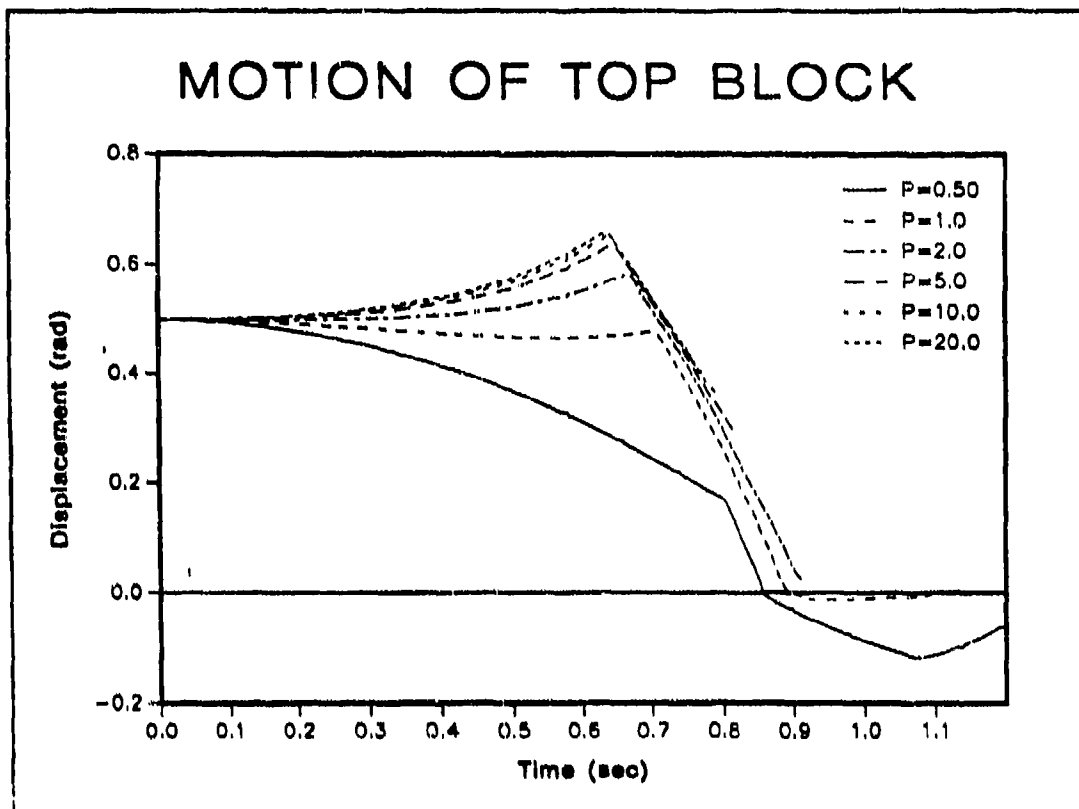
MOTION OF TOP BLOCK

FIGURE 9 - Vibration of Top Block as a Function of the Ratio P

Considering the motion of the bottom block, as seen in Figure 10, it is not surprising to see that as the P ratio decreases the bottom block's motion becomes more gradual and the first impact time lengthens out. This is somewhat intuitive in the sense that it would seem reasonable to expect that motion of the bottom block would quicken as the mass of the bottom block increases. Also, as the mass of the bottom block increases relative to the top block, i.e., an increasing P ratio, the curves in Figure 10 approach an asymptote which appears to coincide with the $K=0$ curve in Figure 8. This is reasonable in that the effect of the mass of the top block on the system response decreases with an increasing P ratio. Figure 10 also shows that once the bottom block impacts, the system motion damps out very quickly. This phenomenon is thought to be caused by the coupling inherent in these type of systems.

The trend in Figure 9 shows that increasing the P ratio causes the displacement of the top block to initially increase rather than decrease. Physically, as the mass of the bottom block increases, the restoring moment due to gravity acting on the bottom block increases, causing the bottom block to rotate down faster. This displaces the point of rocking associated with the top block causing a destabilizing moment on the top block; hence, its displacement angle increases. Figure 9 shows that this displacement increase due to the mass ratio does not grow indefinitely but approaches

38
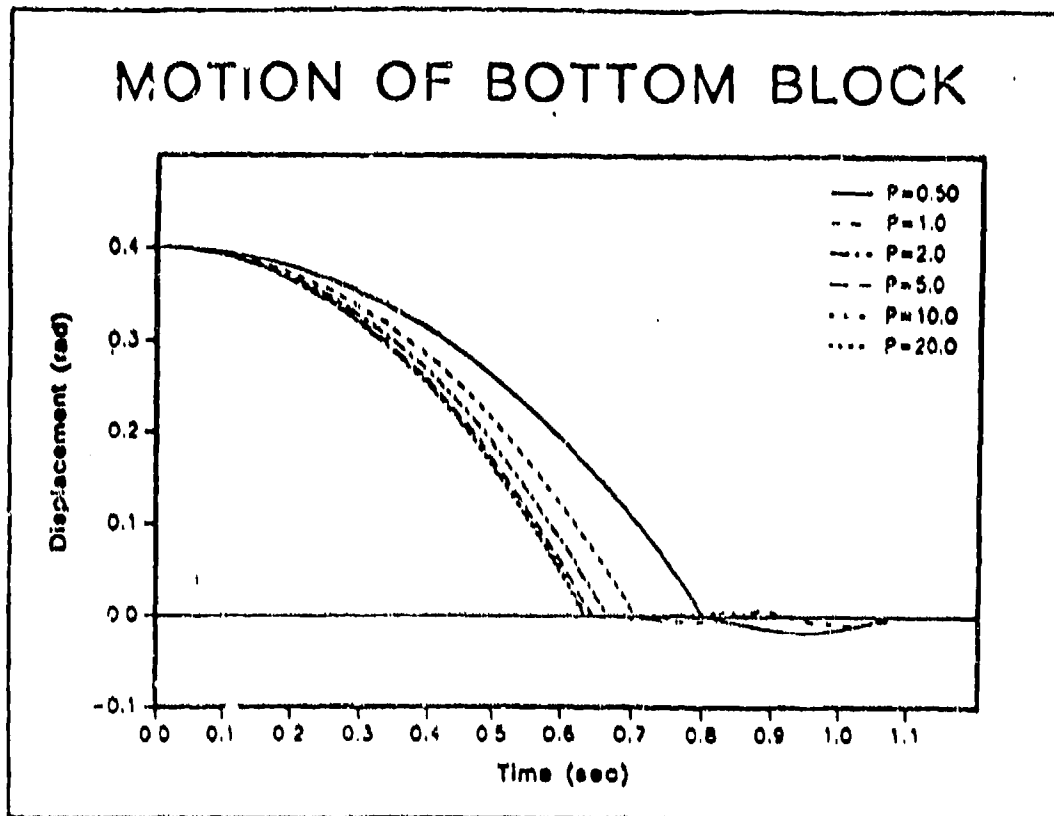
FIGURE 10 - Vibration of Bottom Block as a Function of the Ratio P

a terminal value that is believed to be a function of the physical parameters of the system. Thus, if a stability criterion for the top block was known, then a comparison with this terminal value could address the toppling of the top block.

Since the physical criteria for toppling or system instability for MDOF systems are not generally well defined, no general conclusions can be drawn about the stability of MDOF systems at this time. It is possible to generate mathematical constraints or criteria for stability for the linear regimes of motion in terms of the physical parameters of the problem, but this does not address the issue of system stability because at transition the dynamics of the problem change instantaneously. This discontinuous change has the potential to convert a mathematically unbounded solution to a stable one or a mathematically bounded solution to an unstable solution. One straightforward method to solve this dilemma is to analyze the response of a specific system and see if the time history grows unbounded.

A cursory examination of the dynamic stability of this particular model in terms of how varying the stiffness affects the system response was performed and the results are presented in Figure 11. For this example, two stiffness constants were chosen, $k=0$ lbs/ft and $k=50,000$ lbs/ft. The densities of both blocks were set at 145 lbs/ft and the

39

bottom block had dimensions of $8x8x8 \, ft^3$ while the top block was cubic, also with dimensions of $4x4x4 \, ft^3$. The initial displacements of both blocks were zero with the initial velocities of both blocks as variables to generate the stability plot.

The most important consideration in generating this plot was what stability criteria to use. For the case where the stiffness was zero, i.e., no spring, the top block was considered to topple after passing *45 degrees* in displacement which is the static equilibrium point for a cubic, homogeneous block. It is harder to justify toppling of the bottom block, at the same point for the following reason. If the point of rotation of the top block resting on the bottom block is in the same direction of displacement of the bottom block then the additional weight of the top block would impart an additional destabilizing moment on the bottom block causing toppling to occur sooner than *45 degrees*. Conversely, if the point of rotation of the top block on the bottom block is on the furthest edge of the bottom block, in terms of the bottom block's point of rotation, then the weight of the top block would provide an additional stabilizing moment so that toppling of the bottom block would occur after *45 degrees*. For simplicity, the critical stability point was chosen to be *45 degrees* for both blocks since the primary interest was to account for the effect of the system stiffness on system stability, and not to determine the exact stability state of the system.

FIGURE 11 - Stability as a Function of Stiffness K

40

The stability criteria for the case where the system stiffness is not zero is more complex. In general, the stabilizing and destabilizing moments are functions of both the spring stiffness and the displacement angles, so a simple number criterion could no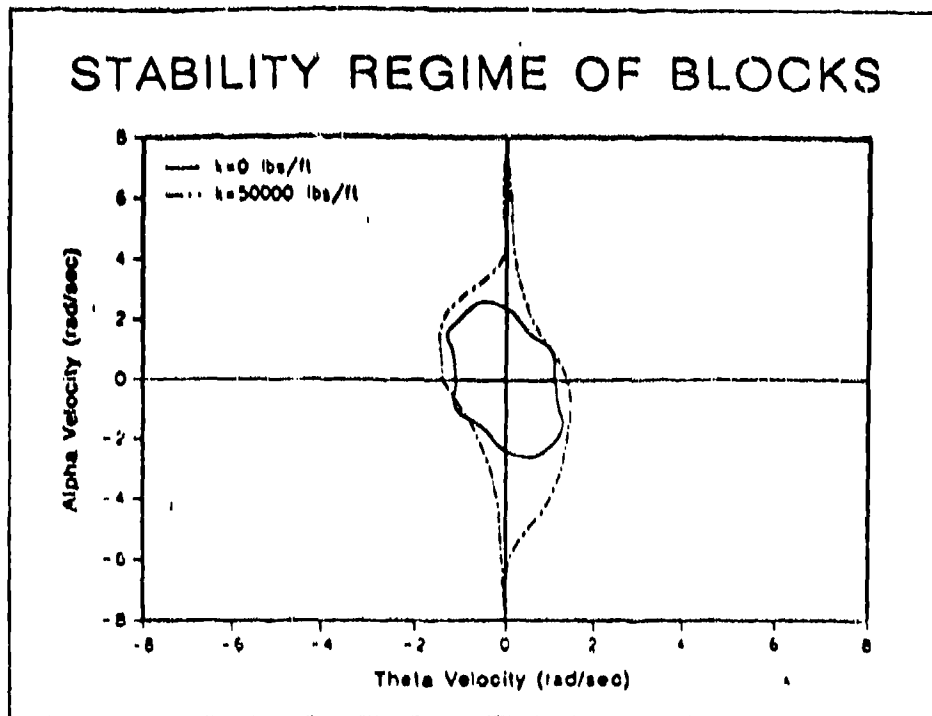t be determined. The system was started and the response of both blocks were examined after the displacement exceeded *45 degrees*. If the solution continued to grow unbounded, then the system was considered unstable with those initial conditions. If the solution became bounded within *5%* of *45 degrees* or transitioned which resulted in a velocity reduction or reversal, then the system was considered stable with those initial conditions.

Some general observations can be drawn from Figure 11. For this 2DOF system, stability is a function of the stiffness and, as the stiffness increases, the region of stable behavior grows larger. The region of stability for both stiffness curves is centered on the origin of the coordinate system which is to be expected, and the shapes of the curves, though not symmetric, have a rough order to them.

The second parametric study of the 2DOF system was to examine what affect variation of the spring stiffness had on the system response. The physical dimensions of the blocks remained the same and the density of both blocks was set at *145 lbs/ft³*. The bottom block was given an initial positive tilt of $\theta_0 = 0.4$ radians and the top block one of $\alpha_0 = 0.5$ radians. Six values of K were used ranging from zero to *5,000,000 lbs/ft* and the blocks were allowed to oscillate freely. The results are presented in Figures 12 and Figure 13, respectively.

Figure 12 illustrates the motion of the top block as a function of six different spring stiffnesses. The general trend is somewhat similar to the SDOF case as shown in Figure 8; that is, as the stiffness of the system increases, the curves shift down and left, leading to quicker impact times. For high values of K, the curves appear to converge to some asymptote and the same first impact time. It is believed that this asymptote is strictly a function of the physical parameters of the system and not the stiffness terms. Also, note that the initial slope of the curves tends to be steeper for the stiffer systems and then level off to the slope of the asymptote. To really understand this system response, Figure 13 must be examined in context with Figure 12.

Figure 13 illustrates that there appears to be little variation in the response of the bottom block with respect to the different K values. As with the SDOF system, it appears that the response of the bottom block is a weak function of the K parameter and primarily a function of the physical properties and initial conditions of the system. A comparison of Figure 13 with the $K = 0$ curve in Figure 8 highlights that the top block has some effect on the motion of the bottom block and for these specific conditions, the effect is relatively small. One must be careful in drawing general conclusions concerning this point because the relative mass ratios of the blocks will confound the analysis of the effect to some degree. When the mass of the top block is roughly equal to or less than the mass of the bottom block, then the first impact of the bottom block is delayed with respect to the SDOF system. Also, the addition of the top block with its inherent coupling effects introduces a synergism to the system such

41

that after the first impact, the system response really dies down due to the energy dissipation associated with the transition equations. This is even seen for 2DOF systems that are so stiff that they can be modeled as one rigid body due to a high spring stiffness, i.e., large values of K.

TIME HISTORY OF TOP BLOCK

Displacement (rad)

0 5

0 3

0 1

-0 1

K = 0 lbs/ft
K = 50,000 lbs/ft
K = 250,000 lbs/ft
K = 500,000 lbs/ft
K = 1,000,000 lbs/ft
K = 5,000,000 lbs/ft

0.0   0.1   0.2   0.3   0.4   0.5   0.6   0.7   0.8   0.9   1.0   1.1

Time (sec)
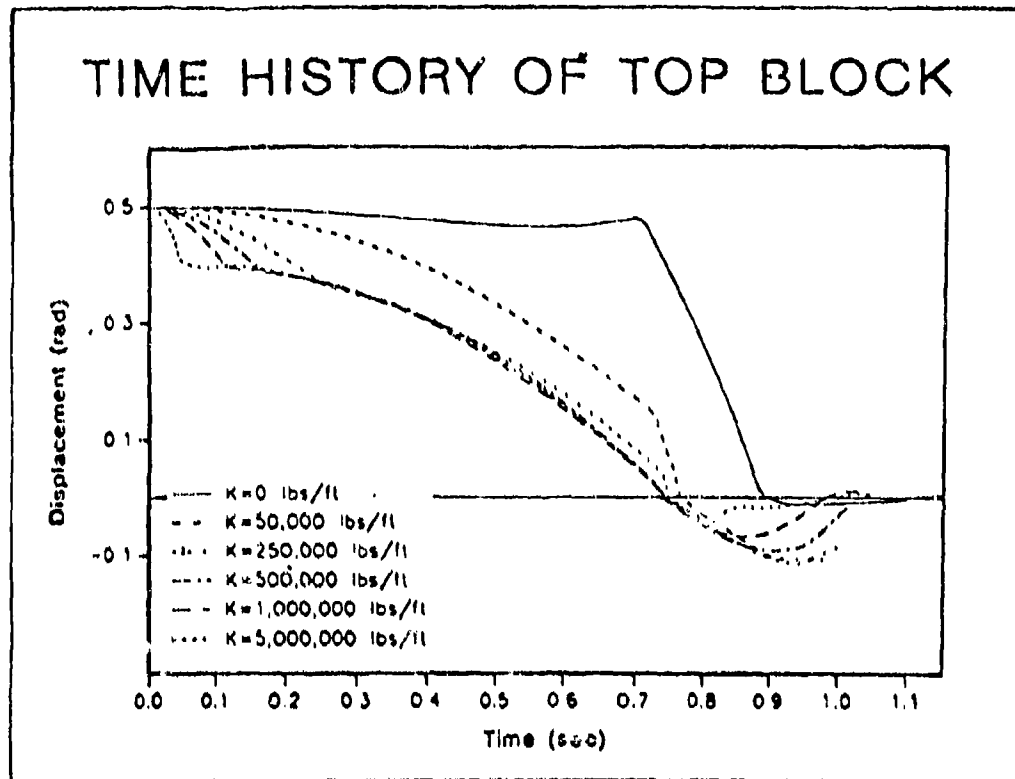
FIGURE 12 - Vibration of Top Block as a Function of Stiffness K

With this understanding, it can be seen in Figure 12 and 13 that as the spring stiffness increases, the system becomes more rigid in nature and begins to respond similarly to SDOF systems. That is the significance of the asymptote discussed earlier in this section. It represents the physical condition where both blocks, though still separated relative to each other, are rocking in concert as if they were a single block. It is evident from Figure 12 that the spring acts to pull the blocks closer to one another, which explains the steepness of the initial slopes for the stiffer systems. The blocks are just approaching each other at a faster rate and it is interesting to note that the asymptotic curve starts at about 0.40 radians or the initial displacement for the bottom block since, in this case, the bottom block is eight times as massive as the top block. Also, the stiffer the system the closer the impact times of each block are to each other. For this example the impact time for both blocks for the stiffest system is approximately 0.74 to 0.75 sec.

42

TIME HISTORY OF BOTTOM BLOCK
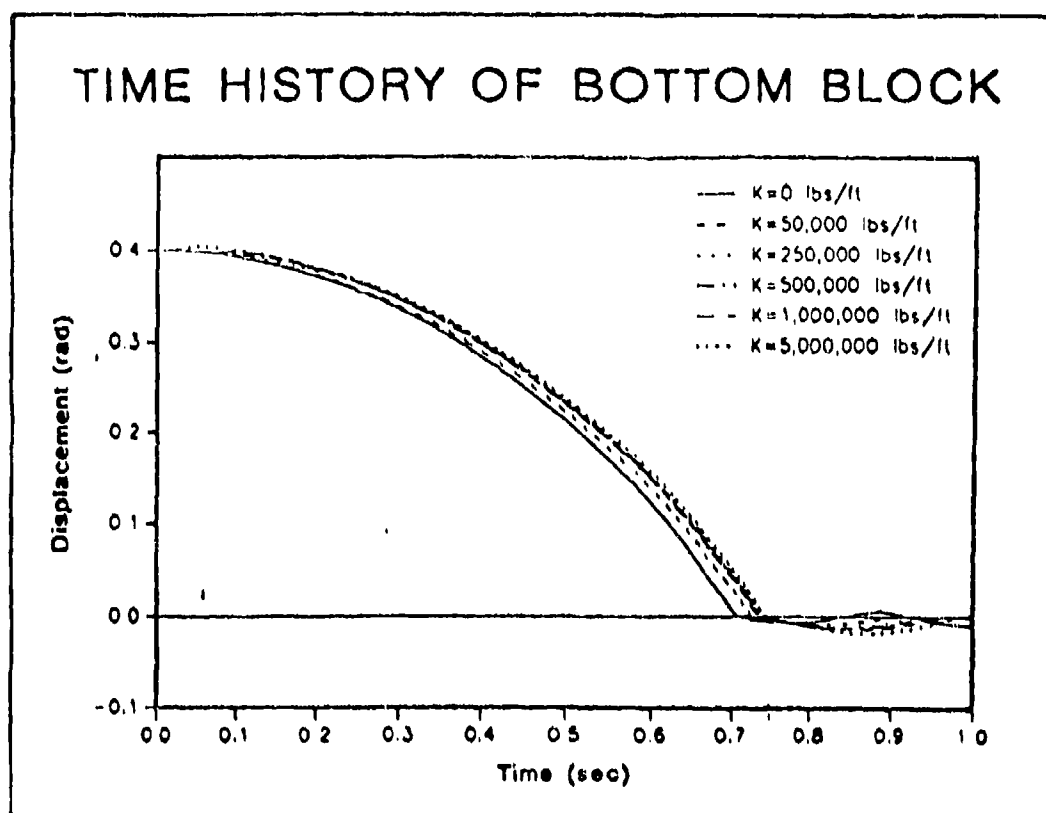
FIGURE 13 - Vibration of Bottom Block as a Function of Stiffness K

For the parameters used to produce Figures 12 and 13, the critical spring stiffness required to cause a change in the character of the solution for each original spring stiffness was determined using equation 32 and is presented in Table 2.

TABLE 2 - 2DOF Character of Solution at Various Stiffness

K (lbs/ft)	K_1 (lbs/ft)	K_2 (lbs/ft)
-5,000,000	91,239,579,585	68,398
-1,000,000	3,841,418,541	70,802
-500,000	1,001,312,068	68,374
-250,000	271,482,930	68,355
-50,000	18,927,269	68,251
0	1,803,504	68,014
50,000	3,084,635	68,857
250,000	192,272,695	68,445
500,000	842,891,734	68,419
1,000,000	3,524,577,939	68,407
5,000,000	91,239,579,585	68,397

43

Table 2 shows that for this specific problem, irrespective of the original stiffness chosen, the critical stiffness K_1 will always be positive and greater than the original stiffness; hence, the generalized solution q_1 will always consist of trigonometric terms only and never change character. However, it is also interesting that the critical stiffness parameter, K_2, appears to be independent of the original stiffness but always positive. The generalized solution, q_2, will change character, from trigonometric terms to hyperbolic terms, for K exceeding approximately *69,000 lbs/ft*. Thus the character of the general solution as presented in equations 29 and 30 , will consist of trigonometric functions below an original system stiffness of 69,000 lbs/ft and consist of a combination of trigonometric and hyperbolic functions above that value for this particular system.

The final topic of this report concerns the constants used in the transition equations 39 and 41 that are strictly functions of the physical parameters of the system modeled. Table 3 presents some values for these constants for various geometries of stacked blocks. Column 2 represents the values for the example problem used here.

Table 3 - C and D Values as a Function of Block Geometry

Block Dimension (HxWxD)	4x6x6 4x6x6	4x4x4 8x8x8	8x8x8 8x8x8	12x4x4 12x4x4
c_1	0.31	0.28	0.75	0.63
d_1	0.65	1.77	0.44	0.63
c_2	0.60	0.97	0.81	0.73
d_2	0.40	0.03	0.19	0.27
c_3	0.81	0.76	0.37	0.54
d_3	0.19	0.24	0.63	0.46
c'_1	1.28	1.02	1.11	1.18
d'_1	-1.17	-1.54	-0.29	-0.52
c'_2	0.72	0.99	0.89	0.82
d'_2	0.28	0.01	0.11	0.18
c'_3	1.17	0.77	0.29	0.52
d'_3	-0.17	0.23	0.71	0.48

Note that the top dimension represents the top block and the bottom dimension the bottom block. Also, the primed constants are the values for the reversed transitions as outlined on pages 26 through 28.

The trend for MDOF systems in general, and for this 2DOF system specifically, is the more slender the system is, the smaller the energy loss during transition. Though the trend is somewhat confounded due to the coupling between the blocks, it is readily evident in constant c_1 which governs the theta transition. Constant d_1, which influences the top block transition, shows that the most significant factor affecting

44

energy loss is the relative block sizes, more so than the geometry of the individual blocks. Constants c_2, c_3, d_2 and d_3 govern the top block transition and no specific conclusions can be drawn from this relatively more complex transition.

To summarize, although 2DOF stacked block systems in general behave in nonintuitive ways as Psycharis [13] showed, the addition of spring connectors to such systems affect the response in a reasonable and predictable manner.

5. CONCLUSION

A dynamic analysis and computer simulation were performed on two simple block systems. The first system modeled was a single block with two attached springs representing fasteners. The second system modeled was two symmetrically stacked blocks connected together by two springs and resting on a horizontal base. Both systems were analyzed for the case of free vibrations, no slip, and perfectly elastic impacts.

The equations of motion were derived using Newton's second law and moment considerations. This problem is nonlinear due to the nonlinear terms in the equations, and also due to the discontinuity associated with the transition from one pole of rotation to the other pole of rotation during impact of the bottom block with the ground and impact of the top block with the bottom block. Thus the system motion was considered in terms of four main regimes of motion where the motion within a regime was continuous and the system motion was piecewise continuous. A linearization process was applied to the four main regimes of motion only and transition equations were developed to account for the physical discontinuity associated with the transition to different poles of rotation. This linearization process enabled the resulting equations to be uncoupled with modal analysis techniques and analytic solutions to be determined. Using this modal analysis technique resulted in independent, second order equations with inertial and stiffness coefficient matrices comprised of geometric and physical parameters only. Thus a parametric study was performed in terms of the mass and stiffness variations.

It is shown that the addition of fasteners, represented as springs of variable stiffness, affect system response in reasonable and predictable ways. The SDOF system behaves as a simple harmonic oscillator between impacts and the addition of a viscous damping mechanism is used to account for the energy dissipation due to the transition.

It is also shown that the response of such a system is a weak function of the stiffness parameter. The 2DOF system also responds in a reasonable fashion. It is shown that the spring stiffness parameter plays no role during transition and is at best, a minimal function in terms of system response. In fact, the system response of the SDOF case is affected more by spring stiffness variations than the 2DOF system.

The methodology used in this report is a viable way to handle the extremely complex dynamical equations developed for these relatively simple cases. In particular, modal procedures enabled analytic solutions to be determined and

46

implemented within a computer code to generate the time histories. This report also illustrated the need for a more in-depth look at transition and its importance to properly account for energy dissipation.

INTENTIONALLY LEFT BLANK.

6.0 REFERENCES

1. Bollo, M.E., "Observations and Implications of Tests on the Cypress Street Viaduct Test Structure," Report No. UCB/GERC-30/21, University of California, Berkeley, 1990.

2. Safak, E. and Celebi, M., "Seismic Response of Transamerica Building I & II," Journal of Structural Engineering, Vol. 117, pp. 2389-2425, 1991.

3. Housner, G.W., "The Behavior of Inverted Pendulum Structures During Earthquakes," Bulletin of the Seismological Society of America, Vol. 53, No. 2, pp. 403-417, Feb. 1963.

4. Psycharis, I.N., "Dynamic Behavior of Rocking Structures Allowed to Uplift," Report No. EERL 81-02, California Institute of Technology, Pasadena, California, August 1981.

5. Yim, C. and Chopra, A.K., "Earthquake Response of Structures with Partial Uplift on Winkler Foundations," Earthquake Engineering and Structural Dynamics, Vol.12, pp. 262-281, 1984.

6. Koh, A., Spanos, P.D. and Roesset, J.M., "Harmonic Rocking of Rigid Block on a Flexible Foundation," Journal of Engineering Mechanics, Vol. 112, No. 11, pp. 165-1180, Nov. 1986.

7. Hogan, S.J., "On the Dynamics of Rigid-block Motion Under Harmonic Forcing," Proc. Royal Society of London, A 425, pp. 441-476, 1989.

8. Koh, A., "Rocking of Rigid Blocks on Randomly Shaking Foundations," Nuclear Engineering Design, Vol. 97, pp. 269-276, 1986.

9. Iyengar, R.N. and Manohar, C.S., "Rocking Response of Rectangular Rigid Blocks Under Random Noise Base Excitations," International Journal of Non-linear Mechanics, Vol. 26, No. 6, pp. 885-892, 1991.

10. Yim, C., Chopra, A.K. and Penzien, J., "Rocking Response of Rigid Blocks to Earthquakes," Journal of Earthquake Engineering and Structural Dynamics, Vol. 8, pp. 565-587, 1980.

11. Ishiyama,Y., "Review and Discussion on Overturning of Bodies by Earthquake Motions," International Institute of Seismology and Earthquake Engineering, Building Research Institute, Ministry of Construction, Japan, June 1980.

12. Lipscombe, P.R., Pellegrino, S., "Free Rocking of Prismatic Blocks," Journal of Engineering Mechanics, Vol. 119, No. 7, pp. 1387-1410, July 1993.

13. Psycharis, I.N., "Dynamic Behavior of Rocking Two-block Assemblies," Journal of Earthquake Engineering and Structural Dynamics, Vol. 19, pp. 555-575, 1990.

14. Allen, R.H., Oppenheim, I.J., Parker, A.R. and Bielak, J., "On the Dynamic Response of Rigid Body Assemblies," Journal of Earthquake Engineering and Structural Dynamics, Vol. 14, pp. 861-876, 1986.

15. Sinopoli, A., "Kinematic Approach in the Impact Problem of Rigid Bodies," Journal of Applied Mechanics Review, Vol. 42, No. 11, Part 2, pp. s233-s244, 1989.

16. Oppenheim, I.J., "The Masonry Arch as a Four-link Mechanism Under Earthquake Excitation," Carnegie-Mellon University, Pittsburgh, Pennsylvania, to be published.

17. Allen, R.H., "A Rigid Body Mechanism in Structural Dynamics," Ph.D. Dissertation, Carnegie-Mellon University, 1984.

APPENDIX A - SAMPLE DERIVATION OF EQUATION OF MOTION

To further illustrate the process, a sample derivation of the equation of motion for case 1 will be shown.
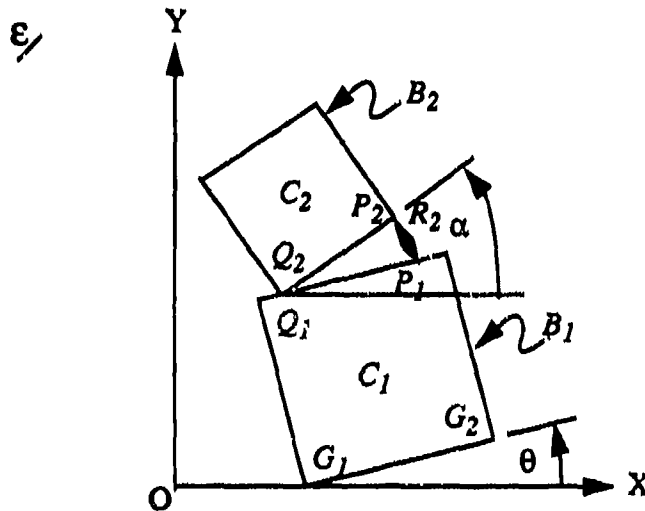
FIGURE A.1 - CASE 1

The equation of motion for the top block was derived first by recognizing that the dynamic moment of block B_2, $\delta(Q_2, B_2/\varepsilon)$ is equal to the sum of the moments of the forces acting on block B_2, with respect to the inertial reference frame ε.

$$\delta(Q_2, B_2/\varepsilon) = M(Q_2, \{\bar{B}_2 \to B_2\}) \tag{A1}$$

Point Q_2 was chosen to simplify the derivation since the contact forces acting on block B_2 act through point Q_2, therefore the moment of those forces are zero at point Q_2. Also the bar symbol above B_2 in the RHS of equation A1 means forces external to B_2, thus the expression $\{\bar{B}_2 \to B_2\}$ symbolizes the forces external to block B_2 that act on block B_2. Now consider the LHS of equation A1 first. By definition,

$$\delta(Q_2, B_2/\varepsilon) = \frac{d}{dt}[\sigma(C_2, B_2/\varepsilon)]\Big|_\varepsilon + r_{Q_2 C_2} \times m_2 g(C_2/\varepsilon) \tag{A2}$$

51

where $\sigma\,(C_2, B_2/\varepsilon)$ is the moment of momentum (angular momentum) of block B_2 about point C_2 with respect to inertial reference frame ε and $g\,(C_2/\varepsilon)$ is the acceleration at point C_2 with respect to reference frame ε. The moment of momentum is defined by equation A3 in general and, for this particular case, results in equation A4 (see Appendix B for more detail on moment of momentum).

$$\sigma\,(A, S/\varepsilon) \;=\; m_S \underline{r}_{AG_S} \times \underline{v}\,(Q_S/\varepsilon) + \underline{I}_S\,(Q_S, S)\,\underline{w}\,(S/\varepsilon)$$

$$\underline{r}_{AQ_S} \times \underline{w}\,(S/\varepsilon) \times m_S \underline{r}_{Q_S G_S} \tag{A3}$$

$$\sigma\,(C_2, B_2/\varepsilon) \;=\; \frac{d}{dt}[I_{B_2 C_2}\dot{\alpha}\underline{z}]\Big|_{\varepsilon} \;=\; I_{B_2 C_2}\ddot{\alpha}\underline{z} \tag{A4}$$

The acceleration $g\,(C_2/\varepsilon)$ is simply determined by equation A5 below.

$$g\,(C_2/\varepsilon) \;=\; \frac{d}{dt}[\underline{v}\,(C_2/\varepsilon)\,]\Big|_{\varepsilon} \;=\; \frac{d^2}{dt^2}[\underline{r}_{O C_2}]\Big|_{\varepsilon} \tag{A5}$$

thus $g\,(C_2/\varepsilon) \;=\; \dfrac{d^2}{dt^2}[-b_1\underline{X} + 2a_1\underline{j} + (b_1 - l_1)\,\underline{i} + x_2\underline{u} + y_2\underline{v}]\Big|_{\varepsilon}$ using

Figure 3 where the coordinates x_2 and y_2 have their origin at Q_2 of block B_2, i.e., equivalent to the parameters n_2 and h_2, respectively. After taking the derivative twice, the resulting expression for acceleration is presented in equation A6.

$$g\,(C_2/\varepsilon) \;=\; ((b_1 - l_1)\,\ddot{\theta} - 2a_1\dot{\theta}^2)\,\underline{j} - ((b_1 - l_1)\,\dot{\theta}^2 + 2a_1\ddot{\theta})\,\underline{i}$$
$$+\; (x_2\ddot{\alpha} - y_2\dot{\alpha}^2)\,\underline{v} - (x_2\dot{\alpha}^2 + y_2\ddot{\alpha})\,\underline{u}$$

So, after making these substitutions into equation A2 and performing the cross product multiplication, the dynamic moment is explicitly presented in equation A6 below.

$$\underline{\delta}\,(Q_2, B_2/\varepsilon) \;=\; \Big[I_{B_2 C_3} + m_2\,(x_2^2 + y_2^2)\Big]\ddot{\alpha}\underline{z} \;+\; 4m_2\,(\ddot{\theta} + \dot{\theta}^2)\,a_1\underline{z}$$
$$+\; m_2\,(\ddot{\theta} + \dot{\theta}^2)\,(b_1 - l_1)\,(x_2 - y_2)\,\sin\,(\alpha - \theta)\,\underline{z}$$
$$+\; m_2\,(\ddot{\theta} + \dot{\theta}^2)\,(b_1 - l_1)\,(x_2 + y_2)\,\cos\,(\alpha - \theta)\,\underline{z} \tag{A6}$$

52

Now, considering the RHS of equation A1, the sum of the moments of the forces acting on block B_2 will be further delineated into contact forces (surface forces) and body forces (in this case, gravitational fields only).

$$M(Q_2, \{\bar{B}_2 \rightarrow B_2\}) = M(Q_2, \{\bar{B}_2 \rightarrow B_2\}^c) + M(Q_2, \{\bar{B}_2 \rightarrow B_2\}^g) \tag{A7}$$

Considering the first term on the RHS of equation A7, the contact forces acting on block B_2 consist of the force generated by the contact with block B_1 at point Q_2 and the spring force R_2 acting on block B_2 at point P_2. Since the moments are taken about point Q_2, the forces acting through this point contribute no moments! The moment at point Q_2 due to the spring force is given by equation A8.

$$M(Q_2, \{\bar{B}_2 \rightarrow B_2\}^c) = r_{Q_2 P_2} \times k_2 r_{P_2 P_1} \tag{A8}$$

where k_2 is the spring stiffness constant and $r_{P_2 P_1}$ is the spring displacement such

that $r_{P_2 P_1} = k_2 [r_{G_1 P_1} - r_{G_1 P_2}] = k_2 [(l_1 + l_2)\underline{i} - (b_2 + l_2)\underline{j}]$ thus,

$$M(Q_2, \{\bar{B}_2 \rightarrow B_2\}^c) = -k_2(l_1 + l_2)(b_2 + l_2) \sin(\alpha - \theta)\underline{z} \tag{A9}$$

Now the second term on the RHS of equation A7 represents the moment of the field or body forces acting on block B_2 which, in this case, is gravity.

$$M(Q_2, \{\bar{B}_2 \rightarrow B_2\}^g) = r_{Q_2 C_2} \times m_2 g = m_2 g (y_2 \sin\alpha - x_2 \cos\alpha)\underline{z} \tag{A10}$$

So substituting equations A9 and A10 into equation A7 gives the correct expression for the sum of the moments of the forces acting on block B_2.

$$M(Q_2, \{\bar{B}_2 \rightarrow B_2\}) = -k_2(l_1 + l_2)(b_2 + l_2) \sin(\alpha - \theta)\underline{z}$$
$$+ m_2 g (y_2 \sin\alpha - x_2 \cos\alpha)\underline{z} \tag{A11}$$

So to get the explicit expression of equation A1, i.e., the equation of motion for block B_2 in case 1, equations A6 and A11 are substituted into equation A1 and slightly rearranged for convenience. The equation of motion is presented in equation A12.

53

$$\left[I_{B_2C_2} + m_2 (x_2^2 + y_2^2) \right] \ddot{\alpha} z + 4m_2 (\ddot{\theta} + \dot{\theta}^2) a_1 z$$

$$+ m_2 (\ddot{\theta} + \dot{\theta}^2) (b_1 - l_1) (x_2 - y_2) \sin (\alpha - \theta) z$$

$$+ m_2 (\ddot{\theta} + \dot{\theta}^2) (b_1 - l_1) (x_2 + y_2) \cos (\alpha - \theta) z$$

$$= -k_2 (l_1 + l_2) (b_2 + l_2) \sin (\alpha - \theta) z + m_2 g (y_2 \sin\alpha - x_2 \cos\alpha) z \quad (A12)$$

Note that this equation differs slightly from equation 13b since the terms on the LHS are grouped differently, and in this derivation, the parameters x_1, y_1, x_2 and y_2 were used in place of n_1, h_1, n_2 and h_2, respectively. However, the equations are mathematically equivalent.

To find the equation of motion for block B_1 the same procedure is used realizing that there is an additional contact force at point Q_1 due to the weight of block B_2 resting on block B_1.

$$\underset{\sim}{\delta} (G_1, B_1 / \varepsilon) = \underset{\sim}{M} (G_1, \{\bar{B}_1 \rightarrow B_1\}) \quad (A13)$$

Solving for the LHS side of equation A13 first and by definition,

$$\underset{\sim}{\delta} (G_1, B_1 / \varepsilon) = \frac{d}{dt} [\underset{\sim}{g} (C_1, B_1 / \varepsilon)] \Big|_\varepsilon + \underset{\sim}{r}_{G_1 C_1} \times m_1 \underset{\sim}{g} (C_1 / \varepsilon) \quad (A14)$$

Utilizing the general expression for moment of momentum results in equation A15.

$$\underset{\sim}{g} (C_1, B_1 / \varepsilon) = \frac{d}{dt} [I_{B_1 C_1} \dot{\theta} z] \Big|_\varepsilon = I_{B_1 C_1} \ddot{\theta} z \quad (A15)$$

The expression for the acceleration term in the moment of momentum equation is,

$$\underset{\sim}{g} (C_1 / \varepsilon) = \frac{d}{dt} [\underset{\sim}{v} (C_1 / \varepsilon)] \Big|_\varepsilon = \frac{d^2}{dt^2} [\underset{\sim}{r}_{OC_1}] \Big|_\varepsilon \quad (A16)$$

or explicitly

$$\underset{\sim}{g} (C_1 / \varepsilon) = \frac{d^2}{dt^2} [x_1 \underset{\sim}{i} + y_1 \underset{\sim}{j}] \Big|_\varepsilon = (x_1 \ddot{\theta} - y_1 \dot{\theta}^2) \underset{\sim}{j} - (y_1 \ddot{\theta} + x_1 \dot{\theta}^2) \underset{\sim}{i} \quad (A17)$$

54

So, after some mathematical manipulations the LHS of equation A13 is,

$$\underset{\sim}{\delta}(G_1, B_1/\varepsilon) - \left[I_{B_1 C_1} + m_1 (x_1^2 + y_1^2) \right] \ddot{\theta} \underset{\sim}{z} \qquad (A18)$$

Now the RHS of equation A13 is the sum of the moments of the forces acting on block B_1 and can be further categorized as surface and body forces, as shown below.

$$\underset{\sim}{M}(G_1, \{\bar{B}_1 \rightarrow B_1\}) - \underset{\sim}{M}(G_1, \{\bar{B}_1 \rightarrow B_1\}^c) + \underset{\sim}{M}(G_1, \{\bar{B}_1 \rightarrow B_1\}^g) \qquad (A19)$$

where

$$\underset{\sim}{M}(G_1, \{\bar{B}_1 \rightarrow B_1\}^g) - \underset{\sim}{r}_{G_1 C_1} \times m_1 \underset{\sim}{g} - m_1 g (y_1 \sin\theta - x_1 \cos\theta) \qquad (A20)$$

$$\underset{\sim}{M}(G_1, \{\bar{B}_1 \rightarrow B_1\}^c) - \underset{\sim}{r}_{G_1 Q_1} \times \underset{\sim}{F}_{12} + \underset{\sim}{r}_{G_1 P_1} \times \underset{\sim}{R}_2 \qquad (A21)$$

where $\underset{\sim}{F}_{12}$ is the contact force on block B_1 due to block B_2 and $\underset{\sim}{R}_2$ is the force due to the spring interface. The spring force is proportional to the relative displacements of both blocks and is given by $\underset{\sim}{R}_2 = k_2 [(b_2 + l_2) \underset{\sim}{u} - (b_2 - l_2) \underset{\sim}{i}]$. The contact force $\underset{\sim}{F}_{12}$ is more complicated and can be found by performing a force analysis on block B_2.

$$\underset{\sim}{F}_{12} - ((b_1 + l_2) \ddot{\theta} - 2a_1 \dot{\theta}^2) \underset{\sim}{i} - ((b_1 - l_1) \dot{\theta}^2 + 2a_1 \ddot{\theta} - k_2 (b_2 \cdots_2)) \underset{\sim}{i}$$
$$+ (x_2 \ddot{\alpha} - y_2 \dot{\alpha}^2) \underset{\sim}{y} - (x_2 \dot{\alpha}^2 + y_2 \ddot{\alpha} + k_2 (b_2 + l_2)) \underset{\sim}{u} - m_2 g \underset{\sim}{Y} \qquad (A22)$$

So utilizing the expression for the spring force and the contact forces (equation A22), in conjunction with equation A20, results in an explicit expression for equation A19.

$$\underset{\sim}{M}(G_1, \{\bar{B}_1 \rightarrow B_1\}) - -m_2 [(b_1 - l_1)^2 + (2a_1)^2] \ddot{\theta} \underset{\sim}{z}$$

$$-m_2 g [(b_1 - l_1) \cos\theta - 2a_1 \sin\theta] \underset{\sim}{z} + k_2 (b_2 + l_2)(l_1 + l_2) \sin(\alpha - \theta) \underset{\sim}{z}$$

$$- m_2 \{[y_2(b_1 - l_1) - 2 x_2 a_1] \sin(\alpha - \theta) - [x_2(b_1 - l_1) + 2 y_2 a_1] \cos(\alpha - \theta)\} \ddot{\alpha} \underset{\sim}{z}$$

$$- m_2 \{[x_2(b_1 - l_1) + 2 y_2 a_1] \sin(\alpha - \theta) + [y_2(b_1 - l_1) - 2 x_2 a_1] \cos(\alpha - \theta)\} \dot{\alpha}^2 \underset{\sim}{z}$$

$$+ m_1 g [y_1 \sin\theta - x_1 \cos\theta] \underset{\sim}{z} \qquad (A23)$$

Now, substituting the expressions for equations A18 and A23 into equation A13, gives the explicit expression for the equation of motion of block B_1.

$$\{I_{B1C1} + m_1 (x_1^2 + y_1^2) + m_2 [(b_1 - l_1)^2 + (2 a_1)^2]\} \ddot{\theta} \, \underset{\sim}{z}$$

$$- m_2 \{ [y_2 (b_1 - l_1) - 2 x_2 a_1] \sin(\alpha-\theta) - [x_2 (b_1 - l_1) + 2 y_2 a_1] \cos(\alpha-\theta) \} \ddot{\alpha} \, \underset{\sim}{z}$$

$$- m_2 \{ [x_2 (b_1 - l_1) + 2 y_2 a_1] \sin(\alpha-\theta) + [y_2 (b_1 - l_1) - 2 x_2 a_1] \cos(\alpha-\theta) \} \dot{\alpha}^2 \, \underset{\sim}{z}$$

$$- [m_1 h_1 g + 2 m_2 a_1 g] \sin\theta \, \underset{\sim}{z} - K_2 (b_2 + l_2) (l_1 + l_2) \sin(\alpha-\theta) \, \underset{\sim}{z}$$

$$= - [m_1 n_1 g + m_2 g (b_1 - l_1)] \cos\theta \, \underset{\sim}{z} \qquad\qquad (A24)$$

APPENDIX B - MOMENT OF MOMENTUM

The assumption of conservation of moment of momentum for the derivation of the transition equations is necessary for the analytic treatment of this problem and to avoid using an arbitrary *"coefficient of restitution"* to account for the energy dissipation during transition. The proof is presented below.

First, derive a general expression for the moment of momentum of some arbitrary rigid body S about an arbitrary point A that can have a velocity relative to the inertial reference frame $\mathcal{E}$ as shown in Figure B.1 below. This is defined by the expression $\mathcal{G}(A, S/\mathcal{E})$ which, by definition, is given by equation B1.

(B1)
$$\mathcal{G}(A, S/\mathcal{E}) = \int_S \mathfrak{r}_{AP} \times \mathfrak{v}(P/\mathcal{E}) \, dm(P)$$
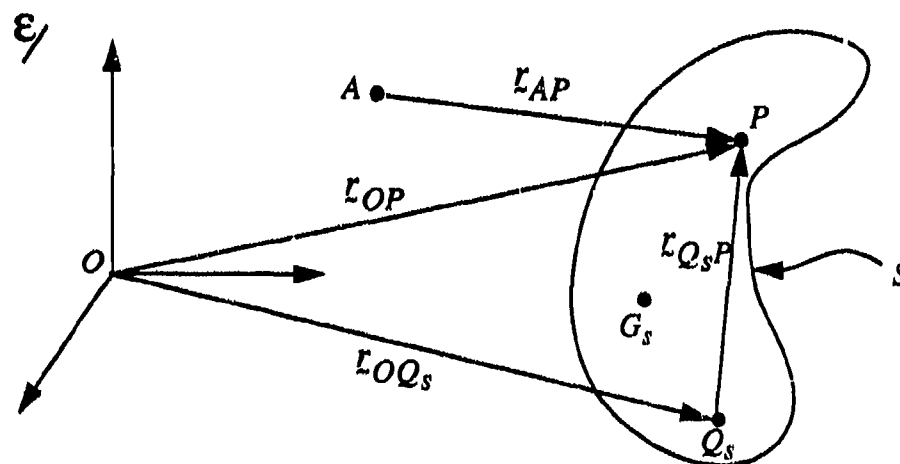

FIGURE B.1 - Moment of Momentum for an Arbitrary Body S

Note that point P is some arbitrary fixed point in S, as is point Q_S, which is some point of body S where the inertial properties, $I_S(Q_S, S)$, are known. Point G_S is the center of mass of body S and the total mass is given by m_S.

Now
$$\underline{v}(P/\varepsilon) = \frac{d}{dt}\left[\underline{r}_{OP}\right]\Big|_\varepsilon - \frac{d}{dt}\left[\underline{r}_{OQ_S}\right]\Big|_\varepsilon + \frac{d}{dt}\left[\underline{r}_{Q_sP}\right]\Big|_\varepsilon$$

where
$$\underline{v}(Q_S/\varepsilon) = \frac{d}{dt}\left[\underline{r}_{OQ_S}\right]\Big|_\varepsilon \quad \text{and} \quad \frac{d}{dt}\left[\underline{r}_{Q_sP}\right]\Big|_\varepsilon = \underline{w}(S/\varepsilon) \times \underline{r}_{Q_sP}$$

so
$$\underline{v}(P/\varepsilon) = \underline{v}(Q_S/\varepsilon) + \underline{w}(S/\varepsilon) \times \underline{r}_{Q_sP}$$

thus
$$\underline{\sigma}(A, S/\varepsilon) = \int_S \underline{r}_{AP} \times \left[\underline{v}(Q_S/\varepsilon) + \underline{w}(S/\varepsilon) \times \underline{r}_{Q_sP}\right] dm(P) \quad \text{or}$$

$$\underline{\sigma}(A, S/\varepsilon) = \int_S \underline{r}_{AP} \times \underline{v}(Q_S/\varepsilon) dm(P) + \int_S \underline{r}_{AP} \times \left[\underline{w}(S/\varepsilon) \times \underline{r}_{Q_sP}\right] dm(P)$$

but
$$\underline{r}_{AP} = \underline{r}_{AG_s} + \underline{r}_{G_sP} \quad \text{and} \quad \underline{r}_{AP} = \underline{r}_{AQ_s} + \underline{r}_{Q_sP}$$

so
$$\underline{\sigma}(A, S/\varepsilon) = \int_S \left[\underline{r}_{AG_s} + \underline{r}_{G_sP}\right] \times \underline{v}(Q_S/\varepsilon) dm(P)$$

$$+ \int_S \left[\underline{r}_{AQ_s} + \underline{r}_{Q_sP}\right] \times \left[\underline{w}(S/\varepsilon) \times \underline{r}_{Q_sP}\right] dm(P) \quad \text{or}$$

(B2)
$$\underline{\sigma}(A, S/\varepsilon) = \int_S \underline{r}_{AG_s} dm(P) \times \underline{v}(Q_S/\varepsilon) + \int_S \underline{r}_{G_sP} dm(P) \times \underline{v}(Q_S/\varepsilon)$$

$$+ \int_S \underline{r}_{AQ_s} \times \left[\underline{w}(S/\varepsilon) \times \underline{r}_{Q_sP}\right] dm(P) + \int_S \underline{r}_{Q_sP} \times \left[\underline{w}(S/\varepsilon) \times \underline{r}_{Q_sP}\right] dm(P)$$

Now for a conservative system, i.e., point P fixed in body S, the displacement vector

$\underline{r}_{G_sP}$ does not vary so $\int_S \underline{r}_{G_sP} dm(P) = 0!$ Also $\int_S \underline{r}_{AG_s} dm(P) = m_S \underline{r}_{AG_s}$

and $\int_S \underline{r}_{AQ_s} \times \left[\underline{w}(S/\varepsilon) \times \underline{r}_{Q_sP}\right] dm(P) = \underline{r}_{AQ_s} \times \underline{w}(S/\varepsilon) \times \int_S \underline{r}_{Q_sP} dm(P)$

58

since r_{AG_s}, r_{AQ_s} and $\underline{w}\,(S/\varepsilon)$ have no dependence on dm(P). Now by

definition, $\quad m_s r_{Q_sG_s} = \int_S r_{Q_sP}\,dm\,(P)\quad$ (def. of mass center)

and the mass moment of inertia is defined as $\underline{I}_S\,(Q_s,\,S)\,\underline{w}\,(S/\varepsilon)$ in equation A3.

(B3) $\qquad \underline{I}_S\,(Q_s,\,S)\,\underline{w}\,(S/\varepsilon) = \int_S r_{Q_sP} \times \left[\underline{w}\,(S/\varepsilon) \times r_{Q_sP}\right] dm\,(P)$

so making these substitutions into equation B2 gives the general equation for moment of momentum, as shown in equation B4 below.

(B4) $\quad \underline{\sigma}\,(A,\,S/\varepsilon) = m_s r_{AG_s} \times \underline{v}\,(Q_s/\varepsilon) + \underline{I}_S\,(Q_s,\,S)\,\underline{w}\,(S/\varepsilon)$

$\qquad\qquad + r_{AQ_s} \times \underline{w}\,(S/\varepsilon) \times m_s r_{Q_sG_s}$

Now, with this general equation, the 2DOF system can be analyzed but the question is how to apply it to the system of interest? At what points and which blocks can the principle of conservation of moment of momentum be applied? Realizing that two independent equations are required to solve the transition problem in closed form and that there are three possibilities - one equation for each block and the system equation - the following proof is offered to show where and how conservation of moment of momentum can be applied to this particular system.

Consider Figures B.2 and B.3 below, which represent a transition from case 1 to case 4, i.e., a θ - transition.
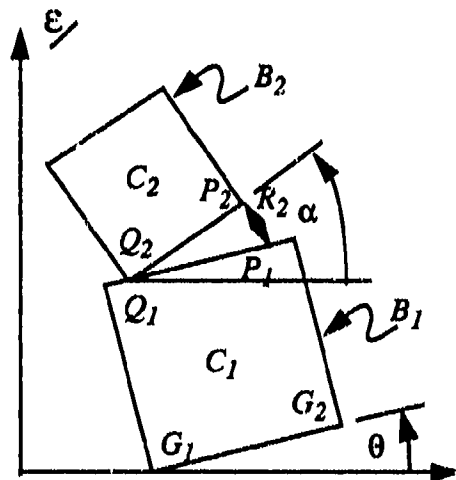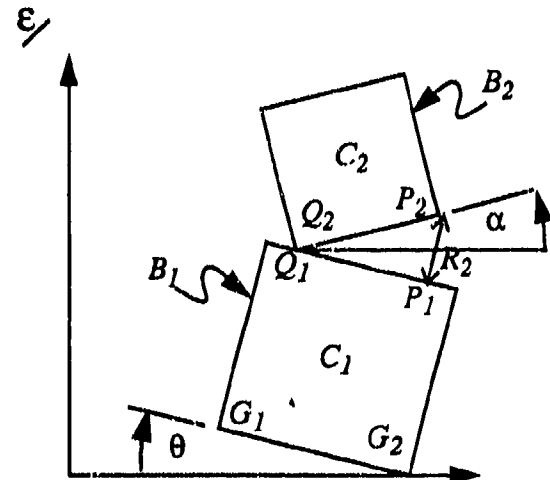

FIGURE B.2 - CASE 1

FIGURE B.3 - CASE 4

Definitions: σ - Moment of Momentum (angular momentum)

ε - Inertial Reference Frame

Σ - System consisting of block B_1 and block B_2 in inertial reference frame ε, i.e., $\Sigma = B_1 \cup B_2$

C_1 - Center of mass of block B_1

C_2 - Center of mass of block B_2

t_i - Time immediately prior to transition

t_f - Time immediately after transition

First consider conservation of angular momentum of the system about point G_2 during transition from case 1 to case 4. For this assumption to be valid, the following condition must be true.

(B5)
$$\sigma\,(G_2, \Sigma/\varepsilon) = constant \qquad as\ \theta \to 0,$$

which is mathematically equivalent to equation B6 below.

(B6)
$$\frac{d}{dt}\big[\sigma\,(G_2, \Sigma/\varepsilon)\big]\Big|_\varepsilon = 0$$

but $\dfrac{d}{dt}\big[\sigma\,(G_2, \Sigma/\varepsilon)\big]\Big|_\varepsilon = \delta\,(G_2, \Sigma/\varepsilon)$ where $\delta\,(G_2, \Sigma/\varepsilon)$ represents the

dynamic moment of the system Σ about point G_2 with respect to reference frame ε.

Now the dynamic moment $\delta\,(G_2, \Sigma/\varepsilon)$ is equal to the sum of the moments about

point G_2 of all the external forces acting on system Σ as shown in equation B7.

(B7)
$$\delta\,(G_2, \Sigma/\varepsilon) = M\,(G_2, \{\bar{\Sigma} \to \Sigma\}) \qquad thus$$

(B8)
$$\frac{d}{dt}\big[\sigma\,(G_2, \Sigma/\varepsilon)\big]\Big|_\varepsilon = M\,(G_2, \{\bar{\Sigma} \to \Sigma\})$$

and integrating this expression from t_i to t_f to get an equation satisfying the condition given in equation B5 results in equation B9.

60

$$(B9) \qquad \mathcal{g}(G_2, \Sigma/\varepsilon) = \int_{t_i}^{t_f} M(G_2, \{\bar{\Sigma} \to \Sigma\}) \, dt = constant$$

But the moments of the external forces can be further delineated into the contact forces acting on the system and the body forces (gravity) as shown in equation B10.

$$(B10) \quad M(G_2, \{\bar{\Sigma} \to \Sigma\}) = M(G_2, \{\bar{\Sigma} \to \Sigma\}^c) + M(G_2, \{\bar{\Sigma} \to \Sigma\}^g)$$

Now since all the contact forces can be considered during impact to act through point G_2, then the moment of those forces about point G_2 are obviously zero. Also during impact, i.e., as $t_f - t_i \to 0$, all of the body forces (gravity) are not varying, thus

$$M(G_2, \{\bar{\Sigma} \to \Sigma\}^c) = 0 \quad \text{and} \quad \int_{t_i}^{t_f} M(G_2, \{\bar{\Sigma} \to \Sigma\}^g) = constant \text{ so}$$

$$\int_{t_i}^{t_f} M(G_2, \{\bar{\Sigma} \to \Sigma\}) \, dt = \int_{t_i}^{t_f} M(G_2, \{\bar{\Sigma} \to \Sigma\}^g) = constant \quad \text{and}$$

conservation of moment of momentum of the system about point G_2 is satisfied!

Now consider conservation of angular momentum for block B_2 about the pole of rotation, point Q_2. The angular momentum of block B_2 about point Q_2 with respect to the inertial reference frame ε is given in equation B11 and comes from the application of equation B4 to this specific case.

$$(B11) \qquad \mathcal{g}(Q_2, B_2/\varepsilon) = m_2 r_{Q_2 C_2} \times \mathcal{v}(C_2/\varepsilon)$$
$$+ I(C_2, B_2) \mathcal{w}(B_2/\varepsilon) + r_{Q_2 C_2} \times \mathcal{w}(B_2/\varepsilon) \times m_2 r_{C_2 C_2}$$

Using equation B4 it is easy to show that:

$$(B12) \quad \mathcal{g}(C_2, B_2/\varepsilon) = m_2 r_{C_2 C_2} \times \mathcal{v}(C_2/\varepsilon) + I(C_2, B_2) \mathcal{w}(B_2/\varepsilon)$$
$$+ r_{C_2 C_2} \times \mathcal{w}(B_2/\varepsilon) \times m_2 r_{C_2 C_2}$$

61

Realizing that $\xi_{C_2 C_2} = 0$, and combining equations B11 and B12, gives

(B13) $\qquad \mathscr{g}(Q_2, B_2/\varepsilon) = m_2 r_{Q_2 C_2} \times \mathscr{v}(C_2/\varepsilon) + \mathscr{g}(C_2, B_2/\varepsilon)$

For angular momentum of block B_2 about point Q_2 to be conserved, the following condition must be true.

(B14) $\qquad \mathscr{g}(Q_2, B_2/\varepsilon) = constant \quad$ during transition

Using the same derivation as for the conservation of angular momentum of the system, the following equation is found.

(B15) $\qquad \dfrac{d}{dt}\Big[\mathscr{g}(Q_2, B_2/\varepsilon)\Big]\Big|_{\varepsilon} = M(Q_2, \{\bar{B}_2 \to B_2\}) \quad$ and integrating

(B16) $\qquad \Big[\mathscr{g}(Q_2, B_2/\varepsilon)\Big] = \displaystyle\int_{t_i}^{t_f} M(Q_2, \{\bar{B}_2 \to B_2\})\, dt \quad$ and as before

$$M(Q_2, \{\bar{B}_2 \to B_2\}) = M(Q_2, \{B_1 \to B_2\}^c) + M(Q_2, \{\bar{B}_2 \to B_2\}^g)$$

and since all of the reaction forces produced during transition pass through point Q_2, the moment of these forces at point Q_2 is zero. Thus

$$M(Q_2, \{\bar{B}_2 \to B_2\}) = M(Q_2, \{\bar{B}_2 \to B_2\}^g) \quad \text{only so equation A16 is}$$

(B17) $\qquad \mathscr{g}(Q_2, B_2/\varepsilon) = \displaystyle\int_{t_i}^{t_f} M(Q_2, \{B_2 \to B_2\}^g)\, dt$

but as $t_f - t_i \to 0$ for transition the body force (gravity) does not vary so

(B18) $\qquad \mathscr{g}(Q_2, B_2/\varepsilon) = \displaystyle\int_{t_i}^{t_f} M(Q_2, \{B_2 \to B_2\}^g)\, dt = constant$

and conservation of angular momentum of block B_2 about point Q_2 is satisfied.

Consider block B_1 and its angular momentum about point G_2, as was done for the system's angular momentum derivation. The system moment of momentum is equal to the sum of the moments of momentum of each of the blocks that comprise the system.

(B19) $\quad \underline{g}\,(G_2, \Sigma/\varepsilon) \;=\; \underline{g}\,(G_2, B_1/\varepsilon) + \underline{g}\,(G_2, B_2/\varepsilon)$

From equation A5, $\underline{g}\,(G_2, \Sigma/\varepsilon)$ = constant, so using the Δ symbol to represent the change in angular momentum as $t_f - t_i \rightarrow 0$ allows the following derivation.

(B20) $\quad \Delta\underline{g}\,(G_2, \Sigma/\varepsilon) \;=\; \Delta\underline{g}\,(G_2, B_1/\varepsilon) + \Delta\underline{g}\,(G_2, B_2/\varepsilon) \;=\; 0$

since the system angular momentum is conserved. Using equation B4 at point G_2, equation B21 can be derived after some manipulation.

(B21) $\quad \Delta\underline{g}\,(G_2, B_2/\varepsilon) \;=\; \Delta\,[\,\underline{g}\,(Q_2, B_2/\varepsilon) + m_2 \underline{r}_{G_2 Q_2} \times \underline{v}\,(C_2/\varepsilon)\,]\quad$ or

(B22) $\quad \Delta\underline{g}\,(G_2, B_2/\varepsilon) \;=\; \Delta\underline{g}\,(Q_2, B_2/\varepsilon) + m_2 \underline{r}_{G_2 Q_2} \times \Delta\underline{v}\,(C_2/\varepsilon)$

but $\Delta\underline{g}\,(Q_2, B_2/\varepsilon) = 0$ from equation B18; therefore, substituting equation B22 into equation B20 results in the correct expression for the change in angular momentum of block B_1 about point G_2 during transition.

(B23) $\quad \Delta\underline{g}\,(G_2, B_1/\varepsilon) \;=\; -m_2 \underline{r}_{G_2 Q_2} \times \Delta\underline{v}\,(C_2/\varepsilon)$

Thus there is no conservation of angular momentum about point G_2 for block B_1!

INTENTIONALLY LEFT BLANK.

2   Administrator
        Defense Technical Info Center
        ATTN: DTIC-DDA
        Cameron Station
        Alexandria, VA 22304-6145

1   Commander
        U.S. Army Materiel Command
        ATTN: AMCAM
        5001 Eisenhower Ave.
        Alexandria, VA 22333-0001

1   Director
        U.S. Army Research Laboratory
        ATTN: AMSRL-OP-SD-TA,
                Records Management
        2800 Powder Mill Rd.
        Adelphi, MD 20783-1145

3   Director
        U.S. Army Research Laboratory
        ATTN: AMSRL-OP-SD-TL,
                Technical Library
        2800 Powder Mill Rd.
        Adelphi, MD 20783-1145

1   Director
        U.S. Army Research Laboratory
        ATTN: AMSRL-OP-SD-TP,
                Technical Publishing Branch
        2800 Powder Mill Rd.
        Adelphi, MD 20783-1145

2   Commander
        U.S. Army Armament Research,
           Development, and Engineering Center
        ATTN: SMCAR-TDC
        Picatinny Arsenal, NJ 07806-5000

1   Director
        Benet Weapons Laboratory
        U.S. Army Armament Research,
           Development, and Engineering Center
        ATTN: SMCAR-CCB-TL
        Watervliet, NY 12189-4050

1   Director
        U.S. Army Advanced Systems Research
           and Analysis Office (ATCOM)
        ATTN: AMSAT-R-NR, M/S 219-1
        Ames Research Center
        Moffett Field, CA 94035-1000

1   Commander
        U.S. Army Missile Command
        ATTN: AMSMI-RD-CS-R (DOC)
        Redstone Arsenal, AL 35898-5010

1   Commander
        U.S. Army Tank-Automotive Command
        ATTN: AMSTA-JSK (Armor Eng. Br.)
        Warren, MI 48397-5000

1   Director
        U.S. Army TRADOC Analysis Command
        ATTN: ATRC-WSR
        White Sands Missile Range, NM 88002-5502

1   Commandant
        U.S. Army Infantry School
        ATTN: ATSH-WCB-O
        Fort Benning, GA 31905-5000

        Aberdeen Proving Ground

2   Dir, USAMSAA
        ATTN: AMXSY-D
                AMXSY-MP, H. Cohen

1   Cdr, USATECOM
        ATTN: AMSTE-TC

1   Dir, USAERDEC
        ATTN: SCBRD-RT

1   Cdr, USACBDCOM
        ATTN: AMSCB-CII

1   Dir, USARL
        ATTN: AMSRL-SL-I

5   Dir, USARL
        ATTN: AMSRL-OP-AP-L

No. of
Copies Organization

<u>Aberdeen Proving Ground</u>

13 Dir, USARL
    ATTN: AMSRL-WT-TB, J. Santiago
            AMSRL-SL-BS,
                R. Grote (328)
                J. Jacobson (328)
                R. Kirby (328)
                D. Petty (328)
                M. Sivack (328) (4 cp)
                E. Quigley (TR#3)
            AMSRL-SL-BA, J. Walbert (1065)
            AMSRL-SL-BG, J. Liu (328)
            AMSRL-SL-B, J. Morrissey (328)

USER EVALUATION SHEET/CHANGE OF ADDRESS

This Laboratory undertakes a continuing effort to improve the quality of the reports it publishes. Your comments/answers to the items/questions below will aid us in our efforts.

1. ARL Report Number ___ARL-TR-504___ Date of Report ___September 1994___

2. Date Report Received _____

3. Does this report satisfy a need? (Comment on purpose, related project, or other area of interest for which the report will be used.) _____

_____

_____

4. Specifically, how is the report being used? (Information source, design data, procedure, source of ideas, etc.) _____

_____

_____

5. Has the information in this report led to any quantitative savings as far as man-hours or dollars saved, operating costs avoided, or efficiencies achieved, etc? If so, please elaborate. _____

_____

_____

6. General Comments. What do you think should be changed to improve future reports? (Indicate changes to organization, technical content, format, etc.) _____

_____

_____

_____

CURRENT
ADDRESS

Organization _____

Name _____

Street or P.O. Box No. _____

City, State, Zip Code

7. If indicating a Change of Address or Address Correction, please provide the Current or Correct address above and the Old or Incorrect address below.

OLD
ADDRESS

Organization _____

Name _____

Street or P.O. Box No. _____

City, State, Zip Code

(Remove this sheet, fold as indicated, tape closed, and mail.)
(DO NOT STAPLE)